DEVELOPMENT AND DEMONSTRATION OF AN AEROSOL TRACER TECHNIQUE BASED ON NEUTRON ACTIVATION ANALYSIS FOR STUDYING CYCLICAL DEPOSITION AND RESUSPENSION OF AEROSOLS FROM SURFACES

FINAL REPORT

Prepared for the California Air Resources Board
Agreement No. 04345

Co-Principal Investigator

Keith D. Stolzenbach

Civil and Environmental Engineering Department
University of California
Los Angeles, CA 90095

Co-Principal Investigator

Arthur M. Winer, Ph.D.

Environmental Health Sciences Department
Environmental Science and Engineering Program
School of Public Health
University of California
Los Angeles, CA 90095

Co-Investigator

Jeong-Hee Lim, Ph.D.

Civil and Environmental Engineering Department
University of California
Los Angeles, CA 90095

Participating Researcher

Cody Livingston
Environmental Health Sciences Department
Environmental Science and Engineering Program
School of Public Health
University of California
Los Angeles, CA 90095

February 20, 2008

DISCLAIMER

The statement and conclusions in the Report are those of the contractor and not necessarily those of the California Air Resources Board. The mention of commercial products, their source, or their use in connection with material reported herein is not to be construed as actual or implied endorsement of such products.

ACKNOWLEDGEMENTS

We thank Professor John Wasson and Dr. Heinz Hubber at UCLA and Professor George Miller at UCI for the use of their facilities and for helping with the analysis of NAA samples. We would also like to thank Dr. Miriam Byrne at National University of Ireland, Galway for helping us with the basic methodology of silica labeling.

We gratefully acknowledge Pastor Jin-So Yoo and the staff at the All Nations Church for the use of the church parking lot and their electronic facilities.

We gratefully acknowledge support for this research by the California Air Resources Board. This report was submitted in partial fulfillment of ARB Agreement No. 04345, "Development and Demonstration of an Aerosol Tracer Technique Based on Neutron Activation Analysis for Studying Cyclical Deposition and Resuspension of Aerosol-Associated Toxic Contaminants," by the University of California, Los Angeles, under the sponsorship of the California Air Resources Board. Work was completed as of August 2007.

TABLE OF CONTENTS

LIST OF FIGURES

LIST OF TABLES

ABSTRACT

A particle tracer methodology based on the use of Neutron Activation Analysis (NAA) to detect concentrations of rare earth elements sorbed to porous silica particles appears to be a promising technique for studying the transport of aerosols and resuspended particulates and the consequent effects on air and water quality and human health. Following an investigation of alternative techniques for labeling, deploying, and recovering the tracer, the feasibility of the NAA methodology was investigated in field experiments designed to measure the resuspension of particles by wind and the resulting deposition on downwind surfaces. All of the basic components of the NAA tracer performed as expected, including the ability of the technique to distinguish between the transport of silica of different sizes labeled with different rare earths. Measured particle resuspension was characterized by rapid initial loss of tracer when first exposed to wind, by a persistent level of tracer sequestered from resuspension, and by almost no dependence on meteorological conditions. The detection of deposited tracer material diluted during transport in the air was severely limited by the level of rare earth labeling achieved in the silica and by higher than expected background levels of rare earth concentrations in silica, sample vials, and natural particulates. The result of this study suggest that the NAA tracer technique can be applied quantitatively at reasonable cost per sample in field scale studies, but that the method is primarily useful in studying particle resuspension from surfaces. The results of the study also indicate that resuspension of particles in the size range used in this study (10 ~ 60 μm) is significant relative to rates of redeposition and that such particles are highly mobile.

1. Executive summary

Background- The importance of atmospheric deposition as a source of trace metal loadings to stormwater runoff is well documented (Garnaud et al., 1999; Davis et al., 2001; Van Metre and Mahler, 2003; Sabin et al., 2006). Studies have also found dry deposition consists primarily of particles of larger than 10 microns in size (Stolzenbach et al., 2001; Lim et al., 2006). The concentrations of these coarse particles are routinely found farther than expected from sources due to resuspension (Sabin et al., 2006; Lim et al., 2006). This leads to the hypothesis that, where a mechanism for resuspension is present, a persistent near-ground layer of contaminant-laden aerosols is constantly deposited and resuspended. In spite of the potential significance of this cyclical deposition and resuspension of toxic substances, almost nothing is known about these processes. Thus the objective of this study was to investigate the feasibility of a tracer technique for quantification of the deposition and resuspension processes.

Methods - The basic methodology applied in this study, developed by Jayasekera et al. (1989, uses Neutron Activation Analysis (NAA) to detect ions of rare earth elements sorbed to commercial porous silica particles that then serve as a tracer analog for natural particulates. In this study, two different particle size ranges, 10 ~ 40 µm and 40 ~ 63 µm, were labeled with two different rare earths, iridium and dysprosium. Following an investigation of alternative labeling, deployment, and recovery techniques, two general categories of experiments were performed. First, particle resuspension alone was studied by deploying a known amount of tracer on an impermeable surface and then sampling the surface over time to determine loss of tracer from the surface due to resuspension by natural wind. Second, the tracer was deployed in a location subject to resuspension by natural wind and then recovered in downwind samples from nearby surfaces. Meteorological data, including wind speed and direction, temperature, relative humidity and barometric pressure, were also measured during each sampling event.

Results - All of the basic components of the NAA tracer methodology performed as expected in this study. The silica spheres functioned well at reasonable cost as the carrier for the rare earth tracer, although the level of rare earth labeling was less than expected and the background level of rare earth concentrations in silica, sample vials, and natural particulates was higher than expected. The extreme cohesiveness of the silica particles made handling difficult, but this was partially solved by mixing the silica with Arizona Dust. In spite of the use of boxes and tents as wind shields, the experimental results imply relatively rapid resuspension of tracer material following exposure to the wind. The experimental results indicate a fraction of the mass of tracer is effectively sequestered from resuspension by wind, even on relatively smooth and impermeable surfaces. Because of the high background levels of rare earth in experimental blanks, the majority of the samples in the deposition experiment were below detection limits. The results of both the resuspension and deposition experiments were essentially independent of the measured meteorological conditions.

Conclusions - The results of this study suggest the NAA tracer technique can be applied quantitatively at reasonable cost per sample in field scale studies, but that, because of modest labeling levels and high background levels of rare earth concentrations, the method is primarily useful in studying particle resuspension from surfaces. The results of the study also indicate that resuspension of particles in the size range used in this study (10 ~ 60 µm) is significant relative to rates of redeposition and that such particles are highly mobile. This finding has significance for the evaluation of health and environmental effects of emitted particulates.

2. Introduction

2.1. Background and problem statement

Urban air generally contains high concentration of toxic contaminants, including organic species, heavy metals and nutrients, mainly due to anthropogenic activities such as industrial and vehicular activities. These toxic materials partition on the particulate phase and are transferred by atmospheric deposition, which is commonly classified as either dry or wet, onto land and water surface. Studies have shown atmospheric deposition can be a major contribution of the total loading to land and water surfaces of organic compounds such as PAHs and PCBs (Datta et al., 1998; Simcik et al., 1998; Franz et al., 1998), trace metals (Yi et al., 1997; Paode et al., 1998; Yi et al., 2001) and nitrogen (Paerl, 1995; Scudlark et al., 1998). A number of recent investigations have concluded an important source of metal loading to urban runoff is atmospheric deposition (Garnaud et al., 1999; Davis et al., 2001; Van Metre and Mahler, 2003). Studies have also found dry deposition is the major contributor to the transfer of airborne toxics and dry deposition consists primarily of relatively large aerosols, larger than 10 microns in size (e.g. Baker, 1997; Stolzenbach et al., 2001).

Recent research on atmospheric deposition by the authors and their colleagues and students has contributed to our knowledge of the sources of toxic substances and the temporal and spatial variations in deposition (Stolzenbach et al., 2001; Lu et al., 2003; Sabin et al., 2006a, Sabin et al., 2006b; Lim et al., 2006). A major finding of this work is that significant concentrations of these coarse aerosols are routinely found farther from sources than would be possible if resuspension were not present, leading to regional rather than local impacts of individual sources. This has lead to the hypothesis that, where a mechanism for resuspension is present, typically traffic or wind, there is a persistent near-ground layer of contaminant-laden aerosols constantly depositing and being resuspended. Toxic substances emitted into the atmosphere from a true original source deposit initially in the vicinity of the source, but are resuspended, and subsequently redeposit and resuspend again. The particulate material generated by the resuspension, often called 'fugitive dust," is estimated to be the major source to the atmosphere of many toxic substances (Watson and Chow, 2000). This process continues until the substances wash-off by rain, or become sheltered from resuspension. Resuspended toxic substances may be a mixture of recently emitted and historically emitted material.

In spite of the potential significance of this cyclical deposition and resuspension of toxic substances, almost nothing is known about the rates and temporal and spatial variations of this cyclical process or about the actual pathways of this material from primary sources to sites of sequential deposition and resuspension. The research reported here was motivated by the need for a technique to quantify the deposition and resuspension processes.

2.2. Previous work

Inference of aerosol transport from measurement of ambient conditions (aerosol concentration, wind speed, etc.) is complicated by the multiplicity of sources for any one contaminant and uncertain levels of background concentrations. To avoid these difficulties, tracers have been used in a variety of studies focused on resuspension and transport of aerosols. Several different substances have been used as tracers for aerosol measurement: phosphorescent zinc sulfide for particle resuspension from an asphalt road (Sehmel, 1973); fluorescent inorganic particulates, zinc-cadmium sulfides for an atmospheric diffusion study (Bierly and Gill, 1963); Lycopodium spores for transport and diffusion of particles (Hay and Pasquill, 1957; Chamberlain,

1967; Clough, 1975). Radioactive rare earth elements are also often used for aerosol studies; examples include iridium (Ir) for size distribution of soot from a fleet of heavy-duty diesels trucks, (Suarez et al., 1998) and technetium tagged into polystyrene particle for deposition of particles to plant and soil surface (Little, 1977).

Jayasekera et al. (1989) developed a methodology that uses neutron activation analysis (NAA) to detect ions of rare earth elements sorbed to commercially available porous silica spheres of known size in the range 1-50 microns. Neutron activation is based on the principle that the activity induced in a material due to bombardment with neutrons is proportional to the mass of material present. A nucleus is irradiated with neutrons from a nuclear reactor via a non-elastic collision, and an excited intermediate is formed. The intermediate will almost instantaneously de-excite into a more stable configuration by emitting gamma rays, and the new configuration may produce a radioactive nucleus that also de-excites (or decays) by emitting gamma rays with a characteristic half-life of the isotope. The different half lives of the isotopes depend on the stability of the excited nucleus, varying from fractions of a second to several years. The emitted gamma rays differ in energy (KeV) with a range of 60 – 200 KeV, and the energy spectrum of emitted radiation is unique to each isotope. The induced activity in a sample of irradiated material is inferred by counting gamma ray emissions as a function of the emission energy. By comparison with the emissions from a known mass of the same material (standard) that was activated and analyzed under the same conditions, the mass of the target element in the sample can be determined

This methodology has been used by several studies employing different rare earth elements. Cesium was used in conjunction with NAA for measurement of resuspension of coarse particles in the Chernobyl region (Wagenpfeil et al., 1999) and for aerosol deposition studies of dysprosium (Dy) (Giess et al., 1994; Byrne et al., 1995; Lai et al., 2002), europium (Shaw et al., 1994), and indium (Byrne et al., 1995). Most of these studies using this tracer technique were confined to wind tunnel or indoor environments rather than full scale conditions.

2.3. Objectives

The overall objectives of this research are:

- To develop and demonstrate the feasibility of the NAA technique and to show its utility in elucidating the transport of fugitive dust and associated contaminants in full scale field environments.
- To show that the NAA technique is capable of detecting and quantifying the transport of surrogate aerosols undergoing deposition and resuspension. Of particular interest is the possibility of using this technique to detect simultaneously tracer particles of different size labeled with different rare earth elements.

3. Experimental Methods and Study Design

3.1. General aspects of experimental design

In applying a tracer to the problem of cyclical deposition and resuspension two general categories of experiments are naturally suggested:

- Resuspension experiment - In this experiment resuspension alone is studied by deploying a known amount of tracer on a test surface, and then sampling the surface

over time to determine loss of tracer from the surface due to resuspension by natural wind. Experiments of this type do not have to deal with the issue of tracer dilution by dispersion.

- Deposition experiment - In this experiment the tracer is deployed on a test surface in a location subject to resuspension by natural wind, and then recovered in samples from surfaces located downwind. This experiment may be limited in spatial scope by dispersion of the tracer.

To minimize the effects of surface conditions, the experiments were performed on impermeable flat surfaces. The following sections discuss the specifics of the experimental design and the methods used in conducting the experiments and in analyzing the results. Specific details for each experimental methodology are presented in section 3.2.

3.1.1. Experimental field site

Both of the categories of experiments performed in this study required a site that had an accessible unobstructed impermeable surface of sufficiently large size that obstacles (trees, buildings, etc.) near the boundaries would not produce highly non-uniform wind patterns. The site selected was the parking lot of the All Nations Church, located at 10000 Foothill Blvd in Lake View Terrace, California (see Figures 1 and 2). The dimensions of this area are about 72 m by 65 m and the area is not obstructed on any side by tall trees or buildings. An agreement with the church guaranteed that the site would be undisturbed during the experiments, which lasted at most 5 days.

3.1.2. Resuspension experiment

The objective of the resuspension experiment was to determine the ability of the tracer technique to measure the time scale of resuspension of labeled particles deployed on the impermeable surface. The deployed particles consisted of two different sizes of silica spheres, 10 ~ 40 microns and 40 ~ 63 microns, labeled with two rare elements, Dy and Ir, respectively. Prior to field placement, the labeled spheres were mixed with Arizona Dust to minimize agglomeration.

This experiment was carried out six times. For each trial, the mixture of labeled particles and dust was deployed on six impermeable test areas, each 20 cm in diameter and spaced a minimum of 3 meters apart (see Figure 3). The total mass of tracer material per unit area was approximately10 g m^{-2}. The test areas were subsequently sampled by vacuuming. The sampling intervals for each time were 0.25, 1, 2, 3, 4 days for the first and the second trial; 2, 4, 6, 8 hours for the third and the fourth trial; and 2, 4, 8, 24 hours for the fifth and the sixth trial. Background, control, and soil sample were also collected. The samples were then transported to UCLA for sample preparation, then to UCI reactor for irradiation followed by analysis at UCLA or UCI. Local meteorological data was also collected during each experimental trial.

3.1.3. Deposition experiment

The objective of the deposition experiment was to determine the ability of the tracer technique to measure particle deposition downwind from a site where labeled particles had been deployed and subsequently resuspended by wind. All deployment and sampling procedures were similar to the resuspension experiment with the exception of the use of surrogate surface deposition plates designed to measure deposition with no subsequent resuspension.

This experiment was carried out three times, one of which included a duplicate set of deployment and measurement sites. The mixture of two sizes of labeled silica with Arizona Dust was deployed in the center of a 20 cm diameter clean area with a total particle mass loading of about 50 g m^{-2}, except for one experiment for which the loading was about 15 g m^{-2}. Six clean test areas for measuring deposition were sited at roughly equal angular intervals on the circumference of a circle centered on the deployment site and having a radius of 1 meter (see Figure 4). This procedure allowed measurement of resuspension and deposition for a full range of wind directions. The deposition plates were deployed next to each deposition test area. All test areas were sampled by vacuuming and the deposition plates recovered 24 hours after the initial deployment. Background and surface control samples were collected during each experiment.

3.2. Experimental procedures

3.2.1. Tracer material

3.2.1.1. Selection of silica spheres

The particles used in this study were porous silica chromatography spheres supplied by Sigma-Aldrich in two size ranges: 10 - 40 μm and 40 - 63 μm. Both size ranges are readily available with an average cost of $108/ 500g. These particles have a pore size of 60 Å. The specific gravity of the spheres was determined to be 2.0 ± 0.06 by adding a known mass of dry silica to a known volume of water, shaking the mixture and letting it stand covered for 24 hours to allow the silica to saturate with water. The density was then computed from the known mass of silica and the observed difference between the final volume of the mixture and the original water volume. The density and size of these particles make them excellent analogs for natural silt and fine sand that comprise a large fraction of resuspended aerosol material (Chow et al., 1992; Lim et al., 2006).

The size distribution of the silica particles was measured using a particle size analyzer (PSS-NICOMP Accusizer 780, Santa Barbara, CA). Although the number distribution of the larger size particles (40 - 63μm) showed a sizeable fraction of particles less than 1 μm, these particles did not contribute significantly to the mass distribution, which was relatively monodisperse on a mass basis (Figure 5). However, the observed size distribution of the particles in the 10 - 40 μm range was polydisperse with no distinct particle size peak (see Figure 6). As described below, sedimentation and decanting technique was used to generate a more monodisperse distribution of the smaller particles by removing the particles less than 10 μm in size.

3.2.1.2. Decanting to improve size distribution

The use of sedimentation as a separation technique is based on the principle that larger particles will settle faster than smaller particles. Approximately 5 grams of silica were added to a 1000 ml cylinder and the cylinder was filled with water to the 1000 ml mark. The top of the cylinder was covered with parafilm. Stirring of the particles was achieved by shaking and inverting the cylinder for one minute. After a given period, a siphon (Tygon tubing) was used to withdraw all water above the 360 ml mark. The withdrawn fluid and the remaining bottom suspension were transferred into beakers for analysis. Size distributions were measured using a particle size analyzer. To perform the analysis, 1:10 dilutions of both suspensions were made and injected into the instrument. The particle size analyzer software (CW 788, Santa Barbara, CA) generated a plot of particle count vs. particle diameter. Observation of the plots indicated the use

of a 3.5 hour settling time was sufficient to generate a relatively monodisperse distribution (Figure 6). Before decantation nearly 80 % of the particles and 26 % or the particle mass were less than 10 µm in size. After decantation, the 48 % of the particles and 12 % of the particle mass were less than 10 µm, producing a narrower size distribution.

3.2.1.3. Mixing with Arizona Dust

Observation of the silica particles used in this study indicated a tendency of the particles to agglomerate due to attractive interactions between the particles. To reduce agglomeration, Arizona Dust, acquired from Powder Technology, Inc, was added to the silica particle mixture (Sehmel, 1973). Arizona Dust is a standard test dust that is manufactured mainly for the purposes of testing filtration equipment. According to the manufacturer, the dust contains particles in the size range of 20 ~ 40 µm, although analysis of the test dust with the particle size analyzer revealed most of the particles were much smaller than 20 µm. Observation of the fine silica particles mixed with Arizona Dust indicated a mixture one third Arizona Dust by weight provided good reduction of agglomeration of the silica particles.

3.2.2. Rare earth selection

The factors to be considered in choosing a rare earth tracer are the background level in nature, detectability by NAA, availability, solubility, half-life of radionuclide isotopes, and cost. For the present study, Dy and Ir were chosen as the target rare earth metals. Ir was chosen as a tracer for this study because it is relatively rare in the earth's crust (0.05 ppb) (Wedepohl, 1995), and has no industrial sources contributing to its atmospheric concentration (Suarez et al., 1998). Additionally, Ir is commercially available as ammonium hexachloroiridate III (41.5 % Ir) for $83.00/g, and is readily soluble in water. The target radionuclide is Ir^{192}, which has a half life of 74 days, allowing enough time to transport and prepare samples for analysis. The reported detectability of Ir is less than 1ng (http://web.missouri.edu/~umcreactorweb/pages/ac_elemlist.shtml). The gamma rays emitted by Ir^{192} have frequencies of 316 KeV and 468 KeV and the neutron activation cross section for Ir^{192} is 9.5×10^{-26} m^2.

Dy has been used widely as an activatable tracer in air particulate studies (Giess et al., 1994; Byrne et al., 1995; Ondov, 1996) because of its low background in nature (3.8 µg g^{-1}) (Wedepohl, 1995), and reasonable material cost of $2.56/g. Dy is also available commercially in a water soluble form as Dy (III) nitrate (37 % Dy) (Alfa Aesar, Ward Hill, MA). The radionuclide for Dy is Dy^{165}, which has a half life of 2.3 hours. The detectability of Dy with gamma detector by NAA is below 1 ng (http://web.missouri.edu/~umcreactorweb/pages/ac_elemlist.shtml). For Dy^{165}, the gamma energy line is 95.14 KeV and the neutron activation cross section is 5.6×10^{-25} m^2. Since Dy has a short half life, rapid transfer systems are used in the counting of its emissions.

3.2.3. Tracer labeling

The methodology for labeling the silica particles with metal salts was developed by Jayasekera et al. (1989). Approximately 5 g of rare earth metal compound was dissolved in 250 ml of DI water, which yields a dissolved concentration of 8 mg ml^{-1}. The solution was then stirred continuously for 6 hours with continuous stirring using a magnetic bar while being heated on a heating plate with a warm temperature of 30 ° C approximately. A mass of 0.5 g of silica particles waw then immersed in 10 ml of the metal salt solution and agitated for about 48 hours by using Wrist Action Shaker (Burrell Scientific, PA). The particles were recovered by filtering using a

Buchner apparatus and rinsing with DI water to remove surface agglomerates. After final filtration the precipitate was dried at 100° C for about 24 hours, and stored in a glass container in desiccators. Prior to the labeling procedure, all sample vials for labeling were cleaned first using 10 % nitric acid followed by rinsing with DI water followed by cleaning with methanol followed by a final rinse with DI water. After cleaning, the sample vials were placed in a positive pressure hood (Air Filtronix, Clifton, NJ) and allowed to air dry.

3.2.4. Blanks, controls, background measurements, and replicates

The mass or concentration of Dy and Ir was measured in the following blanks: unprocessed silica; a small sample vial; Arizona Dust; Mylar used in the deposition plates; filters used in the sample collection; and, local soil samples collected at the edge of the sampling site (see Figure 3).

To determine the effect of the experimental process, the mass of Dy and Ir was measured in samples of silica that had been that had gone through the labeling process but without addition of rare earth salts (process blanks) and in samples of labeled silica that were deployed during the resuspension experiment but were covered by a wind shielded clean Plexiglas box for the duration of the experiment (surface controls).

Prior to deployment of tracer in the resuspension experiments, the particulate material on a few randomly selected test areas was collected by vacuuming to provide an estimate of the background concentrations of Dy and Ir in locally deposited particulate material.

Although the experimental designs for resuspension and deposition includes measurements from duplicate experimental configurations, the number of true replicate samples obtained was limited by the cost of analysis and in some cases by the small mass of material collected. Replicate samples were obtained for samples of Arizona Dust, labeled silica, silica process blanks, surface controls, soil, and background particulate material.

3.2.5. Tracer deployment

3.2.5.1. Preparation of surfaces for tracer deployment

For each experiment, deployment locations were delineated on the asphalt surface using a 20cm diameter sieve and a black permanent marker by tracing the circumference of the sieve on the asphalt. After delineation of the deployment locations, each of the locations was swept with a broom to remove the bulk of background dust or particles that had accumulated on the surface.

3.2.5.2. Wind barriers

Following sweeping of the surface, Plexiglas boxes were then placed over the deployment locations to act as wind barriers during the deployment procedure. Each box consisted of a 38 x 38 cm top panel and three 25 x 38 cm side panels, which left openings on one side of the box and on the bottom. These boxes were oriented to keep the open side of the box downwind of the prevailing wind direction. This procedure was followed to allow the tracer mixture to be deployed from the open side of the box, while at the same time preventing the silica from being blown away during the deployment procedure. In later experiments, a 3-person dome tent was used as an additional wind barrier during the deployment process.

3.2.5.3. Tracer deployment procedure

Resuspension experiments 1 and 2: A measured amount of labeled silica mixture was deployed on the surface of each deployment location. This was accomplished using a sieve (sieve opening of

75µm), which was placed under the Plexiglas box and over the deployment location. A metal spatula was used to remove a premeasured amount (about 0.25 – 0.30 g) of labeled silica mixture from a vial and dispersed over the sieve in a uniform manner (Figure 7). The sieve was then tapped by the spatula to allow the silica particles to fall through the sieve onto the asphalt surface below. This procedure was repeated on each of the deployment locations. After the labeled silica had been deployed on each of the deployment locations, the Plexiglas boxes were then removed from all deployment locations to allow for wind exposure and subsequent resuspension.

Resuspension experiments 3 - 6 and deposition experiments: The deployment procedure for experiments 3 - 6 and the deposition experiments was similar to the procedure for experiments 1 and 2 with the exception that a 3-person dome tent was used as an additional wind barrier during the deployment process in experiments 3 -6. Although the Plexiglas boxes used in experiments 1 and 2 prevented a significant amount of wind interference during the deployment process, it was observed the wind direction was not uniform, which led to noticeable losses of silica during the deployment. A small portion of the polyethylene floor of the tent was removed from the center of the tent to allow placement of the tent over the Plexiglas box, covering the deployment location. The tent could then be entered and the door could be shut to prevent any wind from entering the deployment area (see Figure 8). After mass deployment in a particular location, the tent was moved to the next location for use as a wind barrier. In addition to the tent acting as a wind barrier, the Plexiglas boxes were also modified by closing the open end of the box after mass had been deployed and the tent had been removed. This prevented any wind from entering an individual deployment location while silica was being deployed in other locations. After labeled silica had been deployed in all deployment locations, each of the individual boxes was then removed to allow for wind exposure and subsequent resuspension. Figure 9 shows an example of the final arrangement of sampling surfaces for both experiments.

3.2.6. Tracer collection from surfaces

3.2.6.1. Vacuum recovery system description

The procedure in these experiments for recovering the deployed silica mixture was based on a modified version of the EPA method for determining dust loading on paved surfaces (EPA, 1993). In the EPA method, a portable vacuum cleaner with a preweighed filter bag is used to collect dust from a paved surface. After collection of surface dust, the filter bag is postweighed and a determination of total dust loading is calculated. The vacuum system employed in this experiment consisted of a portable Millipore® vacuum pump connected to a 37 mm Teflon filter (pore diameter = 2.0 µm). To operate the system, a Teflon filter was placed within a plastic 37 mm air sampling cassette and connected to the pump inlet via one quarter inch Tygon® tubing (see Figure 10). The pump flow rate was adjusted to allow air to pass through the filter at a rate of 15 liters per minute.

3.2.6.2. Recovery of silica mixture from deployment surfaces

Preliminary experiments: To gain experience with the recovery system, preliminary deployment and recovery experiments were performed using unlabeled silica at two sites on the UCLA campus, a parking lot with an asphalt surface and a loading dock with a concrete surface. The area of deployment was about 300 cm^2, which is similar to the deployment areas in the resuspension and deposition experiments. One of the purposes of these experiments was to investigate the sensitivity of the mass recovery to the mass loading (mass/area) of the deployment. Accordingly, the mass of silica deployed ranged from 0.1 g to 0.5 g, corresponding to a mass loading from 3 to

15 g m^{-2}**.** Recovery of the mass of silica was performed soon after deployment using the vacuum system described above.

Resuspension experiments: Prior to recovery of the silica mixture, Teflon filters, as described in the previous section, were placed into separate 10.1 cm diameter plastic Petri dishes and were preweighed. Immediately after deployment of the silica mixtures had been accomplished and the Plexiglas boxes had been removed (time = 0 days), one of the Teflon filters from a preweighed Petri dish was assembled into an air sampling cassette and connected to the vacuum system. The deployment location corresponding to time = 0 days was vacuumed until all visible silica particles had been removed. When necessary, the filter was tapped on the side of the cassette directly into the corresponding Petri dish to remove particles from the filter and allow for continued airflow. The Petri dish was covered at all times by a Plexiglas box to prevent loss of the recovered mass from wind during the tapping procedure. After all visible particles had been removed from the surface, the filter was then removed from the cassette and placed into the corresponding Petri dish and capped. The same procedure was repeated for the other deployment locations using Teflon filters and Petri dishes corresponding to different recovery times. After all deployment locations had been vacuumed, the recovered samples were transferred back to the laboratory for post-weight analysis.

Deposition experiments: Teflon filters were removed from Petri dishes, assembled into an air sampling cassette and attached to the vacuum system. Each of the delineated collection areas, including the original area of deployment was vacuumed for approximately two minutes to ensure removal of available silica particles. After vacuuming, the Teflon filters were placed back into the Petri dishes and transported back to the laboratory for analysis.

3.2.7. Deposition plates

Surrogate surfaces for this study consisted of a square of PVC deposition plate, 12 cm by 12 cm in area, covered with a Mylar® sheet coated with a thin layer, approximately 0.089 g, of Apezion L grease (see Figure 11). Prior to sampling, Mylar to be mounted on the deposition plates was cut to the 12 cm by 12 cm, wiped with methanol and soaked in 10 % nitric acid followed by methanol for 5 minutes each, then rinsed with distilled water, and allowed to air dry. Mylar sheets were coated with a thin layer of Apeizon L grease and mounted onto deposition plates, and stored in clean, airtight containers for transport to the field. During sampling, the plate was placed onto the surface putting sticky tape on the back side of the plate to hold firm to prevent moving around in the case of strong wind blowing. After sampling, the Mylar sheets were carefully taken out of the plate, folded inwardly, and placed in a clean Petri dish.

3.2.8. Irradiation

3.2.8.1. Sample preparation

Samples to be irradiated were placed into one of three sizes of polyethylene vials (see Figure 12). The volumes of these vials were 0.27 ml (“SV1”), 8 ml (“SV2”), and 10 ml (“SV3”). Samples from the resuspension experiments were first weighed, and then a measured mass (approximately 80 % of the collected sample mass) was placed into a SV3 polyethylene vial. Because of the smaller amount of mass collected during the deposition experiment, samples from that experiment were treated differently. The Petri dishes which were used for transferring samples from field to the lab were rinsed with a few drops of DI water and the rinsate and the filter were placed into the SV3 polyethylene vials and dried under a Halogen lamp for 24 hrs. The

mylar sheets from deposition plate were folded and also placed into the SV3 sample vials. This sample also required use of a middle sized sample vial (SV2) to hold the Mylar sheet from moving around and to insure it had the same geometry with other samples. All other samples from both the resuspension and deposition experiments, such as background, labeling samples, were placed into the SV1 sample vial.

For the NAA to yield precise quantitative results, it is necessary the activation standard has a similar geometry to the samples. So two different amount of standard were prepared corresponding to sample vial size of SV1 and SV3. The standard samples for NAA analysis were prepared from standard solutions of dissolved salts (1 μg ml^{-1} solutions from Ultra Scientific, North Kingstown, RI) by adding 0.1 ml of standard solution of Dy and Ir onto silica substrates with average mass of 0.02 g and 0.1 g for the SV1 and SV3 vials, which were then allowed to dry under a halogen lamp overnight. The silica used for substrates were the larger particles 10 ~ 40 μm in size. After drying, all of the substrate was placed into the corresponding sample vials.

After samples were placed in vials, the vial inlets were completely sealed off thermally to prevent any spillages after irradiation and wiped with DI water to reduce surface contamination of the sample vial. The sample vials were then bundled into larger sample vials, which were also heat sealed. All the sample vials were transported to the UCI (University of California at Irvine) nuclear reactor (http://chem.ps.uci.edu/~gemiller/reactor.html), and placed into individual cylindrical irradiation capsules.

3.2.8.2. Reactor characteristics

The UCI nuclear reactor is a Mark I TRIGA reactor built by General Atomics, and uses enriched uranium as a neutron source and water and zirconium hydride as a moderator. The reactor operates at a steady-state power of 250 kilowatts. The core of the reactor produces an average neutron flux of 0.8 x 10^{12} neutrons cm^{-2} sec^{-1}.

The reactor is available for an educational purpose and for research or business. Basic reactor charges are $200 per hour and $50 per hour for spectrometer use. For this study, there were 5 reactor visits, and samples were irradiated approximately 3 hours for each visit. The reactor was capable of irradiating 38 samples with a sample vial size of 2.8 cm in diameter. For most of our experiments, the number of samples to be irradiated was more than 38. In order to increase the number of samples per batch, labeling samples, blanks, and controls were placed into smaller sample vials (see next section), five of which could be fitted into a larger sample vials. In this way a total of 190 samples in the small vials could be irradiated. When the smaller sample vials were used, a sixth small sample vial was required to hold firmly five of smaller sample vials to prevent them from moving around inside of the larger vial.

The most important factors in irradiation of the samples are the neutron flux and the irradiation time. By irradiating samples and standards with the same geometry, the need for interpolation between measured efficiency values, correction for coincidence summing, correction for flux gradient across the length of the irradiation container, and accounting for the uncertainty in the gamma-ray emission probability is eliminated (Costrell et al., 1999).

During irradiation the rate of increase R of the number of radioactive atoms is given by

$$R = n\phi\sigma \qquad (1)$$

where n is the number of atoms of target nuclei, ϕ is the neutron flux density (neutrons cm^{-2} sec^{-1}), and σ is the cross section in cm^2. The decay rate is given by

$$D = \lambda N \qquad (2)$$

where N is the product of the activation of the target nucleus and λ is the decay constant of the nuclide (sec^{-1}). The growth in activity is the difference between the growth and decay rate. For given sample characteristics, n and σ, and neutron flux density ϕ, the activity of the sample at the end of the irradiation for a time t, taking into account the decay time after irradiation (T), is given by

$$A = n \phi \sigma (1-e^{-\lambda t}).(e^{-\lambda T}) \qquad (3)$$

The majority of the activity is induced during the first 3-5 times of half-life of the activation product after which activity levels of the product approach a saturation level equal to $n \phi \sigma$. Thus a significantly longer irradiation period does not increase the activity level of the product radionuclide (Ehmann and Vance, 1991). In addition, increasing the irradiation time to more than about two half-lives of the radionuclide causes a corresponding increase in the activity of longer-lived interferants as well.

Although the activity level of the radionuclide can be increased by using a higher neutron flux, this increases the background activity as well as the signal. For increased irradiation time and higher neutron flux, a high-purity quartz glass vial is recommended (Ehmann and Vance, 1991). Accordingly, we used a 3 hours irradiation time and a fixed rate of neutron flux that is set by the operator of the reactor.

3.2.9. Counting

Counting of gamma ray emissions from the irradiated samples was done with hyperpure germanium (HPGe) detectors at both the UCI facility and UCLA. Because of the short half-life of Dy, samples were placed into the gamma ray detector at the UCI facility immediately after irradiation. The Dy samples took less than 5 minutes per sample to count, at a cost of $50 per hour. All samples were then transferred back to UCLA for gamma ray measurement of Ir. The time required to count for Ir-containing samples varied from 5 minutes to 12 hours per sample. Then samples were stored in a contained area for a period of at least two weeks after irradiation. This allowed for decay of short lived isotopes that can interfere with Ir analysis. After gamma ray measurement, all irradiated samples were stored in lead shielded storage until the total activity of all samples reached 0.02 mram hr^{-1} or less, equivalent to the 100 counts min^{-1} necessary for safe disposal.

The gamma ray HPGe detectors at both UCI and UCLA (Canberra, www.canberra.com) are both co-axial models, with a resolution of 1.8 KeV at 1332 KeV. The efficiency of the UCI detector is 25 % and the efficiency of the UCLA detector is 22 %, both of which are in the range of 15-30 % adequate for most NAA applications (Glascock, 1996). The spectral analysis of the activated samples was carried out using a multi channel analyzer and associated software (Genie 2000). A gamma ray spectrum indicates the relative number of gamma counts versus the energy of the gamma rays. A typical spectrum is a series of sharp photopeaks superimposed on a broad, sloping background. Each photopeak represents the decay of a specific radioisotope, although most radioisotopes have more than one photopeak. In an example shown in Figure 13, two

photopeaks of Ir are evident at the energy level of 316 KeV and 468 KeV in addition to peaks associated with several other elements. Dy has one photopeak at an energy level of 95.14 KeV.

To calculate the mass M_{sam} of an element in a sample a "comparator method" was used in which the activity A_{sam} of the sample derived from the gamma ray spectrum of the sample is compared with the activity A_{std} of a standard containing a known mass M_{std} of the element of interest that was irradiated at the same time as the sample. The neutron flux, cross sections, irradiation times, and all other variables associated with counting are assumed to be the same for both the sample and the standard. The equation used to calculate the mass of the unknown sample is (Ehmann and Vance., 1991)

$$M_{sam} = M_{std} \frac{A_{sam} e^{-\lambda T_{sam}}}{A_{std} e^{-\lambda T_{std}}} \qquad (4)$$

where T_{sam} and T_{std} are the decay times after irradiation of the sample and standard, respectively.

The activities of the samples and standards were determined from the gamma ray spectrum using the total peak area (TPA) method in which a straight line is drawn between the beginning and ending channel of the peak and the trapezoid below is subtracted from the gross peak area (Huber, 2003). The activity is then assumed to be proportional to the area of the peak determined in this manner and the ratio A_{sam}/A_{std} in Equation 4 is then simply the ratio of the peak areas. Since Ir has two gamma ray emissions of 316 KeV and 468 KeV, the peak area of two regions should show similar results. For the data analysis, the concentration determined from the signal at 316 KeV was used, because the signal of Ir is stronger at 316 KeV.

In some samples, photopeaks of other elements interfered with the photopeak of the target isotopes, causing errors in the estimated peak area of the emission spectrum of the target isotopes by producing another peak within a certain background range. For example, Figure 14 shows the spectrum obtained from a soil sample which has many multiple peaks that interfere with the Ir signal at the energy level of 316 KeV. Cr^{51}, which has a half life of 27.7days and energy level of 320 KeV, is the likely source of the interfering peak at 316 KeV. Since the gamma ray spectrum consists of a large number of channels in each of which are accumulated, all those counts which fall within a small energy range, this error can be reduced by extending the background region by manually increasing the number of channels (Gilmore and Hemingway, 1995). An example of this procedure for a soil sample is in Figure 14. Before extending the background region, the area of the peak is 7321 with a one standard deviation error of 1.96 % in the peak area calculation. After resetting the background region, the area of peak becomes 33216 with 0.79 % error. After this adjustment, the calculated mass of Ir in the sample of soil changed significantly from 0.00067 µg to 0.0031 µg.

For this reason, any samples for which the counting procedure indicated a coefficient of variance larger than 10 % in Ir concentration were analyzed manually by extending background regions. This procedure was also applied to samples with soil, blanks, Arizona Dust, deposition plates, and background samples. For Dy, the samples did not show photopeak interference at the energy level of 95.14 KeV. However most of the Dy samples were analyzed manually due to their lower mass, resulting from the short half life of Dy (2.3 hrs), lower Dy contents in the samples, shorter counting time, and higher background levels. Although manually analyzed, some of the samples still showed non-detection levels of Dy or Ir.

All blanks contained quantities of the target rare earth metals above detection limit, so all samples were corrected for levels measured in their respective blanks using the following expanded version of equation 4.

$$M_{sam} = (M_{std} + M_{vial} + M_f + M_{dp}) \frac{A_{sam} e^{-\lambda T_{sam}}}{A_{std} e^{-\lambda T_{std}}} - (M_{vial} + M_f + M_{dp}) \qquad (5)$$

In this equation M_{vial}, M_f, M_{dp} are the masses of rare earth detected in the sample vial, Teflon filter, and the Mylar sheet for deposition plate, respectively, for each sample.

3.2.10. Meteorological data

Meteorological data, including wind speed and direction, temperature, relative humidity and barometric pressure, were also measured during each sampling event for both the resuspension and the deposition experiment using a portable meteorological station (PortLog, Rain Wise, Inc.) (see Figure 15). The solar panel of the portable meteorological station was set toward to South with a panel angle of 44 degrees, which is determined from the approximate latitude of the Los Angles region, and the direction was determined using a compass. The meteorological station was located approximately 50 m away from the 210 freeway (northwest corner of sampling location) with a height of 2 m. The station was battery powered, and recorded data at 10 minute intervals. All the samples were collected during dry periods.

4. Results and Discussion

4.1. Tracer material

The silica spheres, with the small fraction removed by decantation when necessary, functioned well at reasonable cost as the carrier for the rare earth tracer. The extreme cohesiveness of the silica made handling difficult, but this was partially solved by mixing the silica with Arizona Dust. It is possible that the variability in rare earth labeling is in part a result of the wide size distribution of the silica. However, obtaining an initially narrower size distribution greatly increases the cost of the spheres.

4.2. Rare earths

The rare earth elements Dy and Ir chosen for this study performed as expected except for several important aspects. First, as discussed below, the labeling procedure did not result in labeled concentrations of rare earth as high as reported in previous studies. It is possible that a different rare earth could have more favorable labeling characteristics. Second, it is reported (http://web.missouri.edu/~umcreactorweb/pages/ac_elemlist.shtml) that the detection limit by gamma detector by NAA for both Dy and Ir are below 1ng. However, as discussed below, the detectability of Dy and Ir in this study, computed from reported counting errors and comparison of replicate samples, is on the order of 10-100 ng for both rare earths. Third, and most important, the background level of both rare earths is surprisingly high in the silica, Mylar, filters, and soil. This high background, coupled with the lower labeling level, imposes a limit on the allowable tracer dilution.

4.3. Labeling

The mean levels of labeling of Dy and Ir obtained in this study are 1900 µg Dy per gram of silica and 43 µg Ir per gram of silica, respectively (Table 1). The labeling yield of Ir is 30 to 40

times lower than reported for other rare earths, while Dy is about the same magnitude as previous studies (Jayesekera et al., 1995). Lim (2006) investigated several different combinations of heating and labeling, and found that preheating the silica followed by a single labeling yielded only half the level of labeling as heating between two labeling steps. Prior to selection of a labeling method for this study, trials were run in which after an initial labeling the silica was heated at a temperature of 500° C prior to second the labeling procedure. This increased the labeling yield slightly, but required intensive labor for preparation and labeling. Although it was decided not to include a heating step in this study, it may be that heating during the labeling process could increase the labeling yield.

4.4. Blanks, Controls, Background concentration, replicates, and analysis errors

For both Dy and Ir, comparison of the unprocessed silica blanks and the process silica blanks (Table 1) indicates no significant contamination occurred during labeling process in the laboratory. The Ir content in the local soil sample and Arizona Dust were 0.02 $\mu g\ g^{-1}$ and 0.03 $\mu g\ g^{-1}$ respectively, which is higher than the Ir concentration of 0.05 ppb in the crust, probably because of urban sources of Ir. The Dy content in the soil and Arizona Dust were 3.6 $\mu g\ g^{-1}$and 1.5 $\mu g\ g^{-1}$, respectively, which are the same magnitude as the crustal value of Dy of 3.8 $\mu g\ g^{-1}$. The rare earth content in the sample vials was small, but large enough to require the corrections applied in the processing of the counting data.

Average background levels of rare earths in samples from test areas were 1.65 $\mu g\ g^{-1}$ and 0.005 $\mu g\ g^{-1}$ for Dy and Ir, respectively (Table 3). These background values are the same magnitude with other blanks. For the levels of Dy and Ir labeling achieved, the rare earth concentration in a mixture of labeled tracer and background material will be at background values for dilutions of about 10^3 for both Dy and Ir. The high background levels thus impose sever constraints on experimental applications in which the tracer material must be detected at dilutions larger than 10^3.

Information on the inherent variability in the analysis processes was obtained by examining the percentage error reported by the gamma counting software and the average percentage difference in replicates as a function of the detected mass of Dy or Ir (see Figures 16 and 17). These results indicate the minimum detectable mass of Dy and Ir are both on the order of 0.01-0.1 μg.

4.5. Deployment and Resuspension issues

4.5.1. Deployed and recovered mass of silica, Arizona Dust, Dy, and Ir

The mass of deployed and collected silica, Dy, and Ir are summarized in Tables 4 and 5 for the resuspension and deposition experiments. For both experiments the material deployed consisted of a mixture of equal masses of Arizona Dust, silica labeled with Dy, and silica labeled with Ir. The computed recovery percentage for total mixture mass, Dy, and Ir and the area normalized deposition rate are also contained in these tables.

For the resuspension experiment the mean deployed mixture mass and recovery percentage were 0.27 g and 57 %, respectively. The mass of both Dy and Ir labeled silica in the mixture was approximately 0.09 g, resulting in an average of 160 μg of Dy and 4.4 μg of Ir. Recovery percentages for both rare earths varied from 8.6 % to 77 %. The variation of recovery rate with time, which is potentially an indication of tracer resuspension, is discussed in detail below.

4.5.2. Deployment issues

One of the challenging procedures for these tasks was the deployment of the mixed silica particles onto the asphalt surface. Two objectives during the procedure were to transfer particles to the surface while minimizing losses and to deploy the particles in a uniform manner across the surface. The deployment procedure used for these tasks had certain limitations that should be investigated in future experiments.

In regards to the first objective, effort was made to reduce the loss of particles as they were transferred from the vials to the surface and from the sieve to the surface. As mentioned previously, Arizona Dust was mixed with the silica particle mixture to prevent the agglomeration of particles. This was necessary to ensure the particles had the ability to fit through the mesh openings in the sieve. In addition, this facilitated the deployment of the particles through the sieve in a uniform manner. Although the presence of Arizona Dust did reduce the degree of agglomeration, there was still evidence of agglomerated particles based on visual inspection. Such particles were crushed with a spatula after it was found they could not pass through the sieve.

Plexiglas boxes were used in all experiments to prevent wind resuspension as the particles were being deployed. In addition to the boxes, it was found that a three-person dome tent was necessary to prevent losses from wind resuspension during the deployment process. This became evident after the first set of experiments where visible wind resuspension occurred during the deployment procedure. After the dome tent was purchased, visible resuspension of particles did not occur. However, the tapping of the spatula may have caused some of the particles to be resuspended prior to landing on the sieve surface. There was also the issue of particles sticking to the sieve as the particles fell through the mesh screen. Although there was no visual sign of such an occurrence, it can be inferred there was some small loss of particles to the sieve as they passed through the screen. The actual losses from particles sticking to the screen should be investigated more thoroughly so that the amount of particles actually reaching the surface can be more accurately quantified.

The second objective, generating a uniform distribution of particles on the asphalt surface, was difficult to achieve in these experiments. As described previously, a metal spatula was used to remove labeled silica from the transfer vials. The spatula was then tapped to allow the particles to fall on to the sieve surface. The small amount of silica used in these experiments did not allow a uniform layer of silica to be achieved on the sieve surface. As a result, small piles were generated on the sieve rather than a uniform layer (See Figure 18). After the sieve was shaken to allow the particles to fall through, small piles of silica particles were also created on the asphalt surface. The nature of the asphalt surface also made it difficult to achieve a uniform layer. Since the surface was rough, piles of silica tended to accumulate on sections of the asphalt where crevices were present. A uniform layer of particles was therefore not achieved in such cases.

4.5.3. Recovery issues

The ability to recover particles from the asphalt deployment surfaces affected the calculated recovery fractions for each of the experiments. As described previously, a 37 mm Teflon filter and pump were used for recovery of the silica particles after deployment. A flow rate of 15 liters $min.^{-1}$ was used. This flow rate was chosen because it was the maximum flow rate that could be accurately achieved with the filter attached to the pump. The main objective of the recovery procedure was to recover all particles remaining on the asphalt surface after deployment.

The primary limitation to the vacuum system was the inability to recover silica particles that had been sequestered on the asphalt surface. The rough nature of the asphalt resulted in the accumulation of particles in crevices on the surface, which sequestered them from both wind and the vacuum. Although the majority of the particles were visibly removed by the vacuum pump, there was still some visible accumulation of particles in the crevices. Such particles could not be recovered and decreased the total recovery fraction.

The results of the preliminary experiment on recovery system clearly demonstrate the role of surface characteristic in determining the recovery rate (Figure 19). Although the percent recovered increased as the deployed mass increases for both the concrete and asphalt surfaces, the recovery was approximately 20 % higher on the smoother concrete surface. The preliminary asphalt recovery results were consistent with the t = 0 measurements and the surface control blanks in the resuspension experiment (Figure 19).

In addition to losses from sequestration, there were also losses due to the adhesion of particles to the vacuum system surfaces, most notably the plastic cassette and the Teflon filter. Efforts were made to remove all visible particles from the cassette and filter surfaces prior to the transfer of the particles to Petri dishes. The loss of particles due to adhesion to the filter was more significant in the resuspension experiment since the filters used in the deposition experiment were sent to the nuclear reactor without any attempt to remove the particles from the filter. As a result there were no adhesion losses to the filter in the deposition experiment. However, both tasks were subjected to adhesion losses on the plastic cassette. In addition, the plastic Petri dishes also provided a source of adhesion loss for the particles. After particles had been placed in the Petri dishes and post-weighed, it was necessary to transfer the particles in the Petri dish to polyethylene vials for transport to the nuclear reactor. Since it was not possible to remove all particles from the dish, such losses potentially decreased the calculated total recovery fraction.

Wind may have also had an effect on the total recovery fraction, especially when the recovery blanks and samples at time = 0 seconds were collected. Although these samples were immediately recovered after the Plexiglas boxes were removed, the small amount of time between removing the box and collecting the sample presented the possibility of wind removal during the recovery procedure. Collecting these samples required approximately one to two minutes. However, during that time, wind may have been able to remove a small portion from the surface as it was collected. As a result, the calculated total recovery fractions could have been decreased.

The results of the recovery blanks and time = 0 samples clearly demonstrate the effects of losses due to sequestration, adhesion, and wind. Specifically, there was a large range of recovery fractions for the blanks in each of the experiments, indicating the effect of each loss process varied for each experiment.

4.6. Resuspension experiment

The purpose of the resuspension experiments was to assess the capability of the tracer technique to quantify the resuspension of deposited material. This resuspension should be reflected in changes in the mass of tracer recovered over time at locations with identical initial quantities of tracer material and exposed to identical environmental influences (wind, etc.). Recovery fractions for Dy and Ir are summarized in Table 4 and presented graphically in Figures 20 and 21.

The mass of tracer recovered in the first samples (time =0) is significantly less (average of 56 %) than the deployed mass for the reasons discussed in the preceding section. This finding indicates either that tracer material was lost during the deployment process or in a very short time after the protective boxes was removed and before the surface was sampled or that the recovery efficiency is low and variable. The experimental design did not include a sample taken inside the tent immediately after deployment, so it is impossible to say when the material was actually lost.

Samples taken after the initial samples do not show a consistent pattern of decreasing mass with time as would be expected if resuspension were present and other factors were negligible. In fact, in several instances the mass recovered is greater at later times. Because all sampled locations were exposed to the same wind regime, this variability in recovered tracer mass must be the result of of variable recovery efficiency, either because of sampling error or because of differences in the surfaces upon which the tracer was deployed.

In spite of the unexplained variability of the recovered tracer mass at later times, the plotted data do suggest a general trend of decreasing recovered mass with time. To investigate this trend, the recovery percentages at each time were pooled and compared statistically with the pooled initial samples. A t-test of these pooled samples indicates that at most of the later times at which samples were taken the later samples are significantly lower than at the initial times. Samples taken at later times were statistically similar to each other ($p>0.5$)**.**

One of the strengths of the NAA methodology is the potential to quantify the difference in transport between particles labeled with different tracers. A paired t-test of all samples from the resuspension experiment indicates clearly that the average recovery rate (37 %) of the smaller Dy labeled particles is significantly ($p<0.001$) greater than the recovery rate (24 %) for the larger Ir labeled particles. A regression analysis of the recovery rates of Dy and Ir indicates they are correlated, with $r^2 = 0.92$ and a slope of 0.61. This result indicates the smaller silica particles were more likely to be resuspended than the larger silica particles, a result consistent with basic concepts of particle resuspension.

One of the most interesting features of the measured recovery percentages is that the recovered mass appears to have a minimum value on the order of 10-20 % of the deployed mass regardless of how much time has passed since deployment. The lowest recovered percentage of total mass is 16.1 % for total mass, 6.3 % for Dy, and 8.7 % for Ir. This indicates a fraction of the mass of tracer is effectively sequestered from resuspension by wind, even on a relatively smooth and impermeable surface. This result has implications for assessing the fate of deposited material over time.

Measured recovery percentages show no significant dependence on measured wind speed and direction ($p<0.001$). This is not surprising considering the high variability in the recovery percentages and the relatively small differences between the mean wind speeds on the different test days.

Paired t-tests were performed to see if the rare earth mass in surface controls, which deployed on a surface and stayed throughout the whole sampling period in the wind shielded box, and the mass of rare earth at time=0 hrs were statistically different, and the result does not show any significant difference ($p>0.25$). This result indicates weathering and sequestration on asphalt was not the major factors affecting on recovery of rare earth elements in this study.

4.7. Deposition results

The purpose of the deposition experiment was to assess the ability of the technique to quantify the deposition of particles originating from an upwind source. In this experiment the upwind source was the resuspension of particles from a test area identical to that used in the resuspension experiment. The recovery percentages are generally higher than observed in the resuspension experiment. Table 5 also contains the absolute and area normalized values for mass recovered at the six downwind sites for both the deposition plates and the impermeable asphalt surface. The majority of these values have been labeled as non-detects because they are smaller than the blank values obtained for this experiment. For this reason, no further attempt was made to interpret these data in terms factors such as dependence on meteorological conditions, differences between the asphalt and surrogate surfaces, etc.

Some information about deposition processes can be inferred from the recovery of total particulate mass on the central test area (denoted by "M" in Table 5) and on the six deposition test areas. The average total particulate mass collected on the deposition sites is 0.026 g, which is about 6% of the average loss of material from the central test areas (0.43 g). In comparison, the average mass of Dy (Ir has too few detected values to be included in this calculation) recovered in the deposition test areas (0.05 μg) is about 0.01 % of the average loss of Dy (606 μg) from the central test area. In addition, the area normalized values for Dy and Ir are generally less than the background area normalized values measured near the experimental test sites (Table 3). These results indicate measured masses recovered from the downwind sites were probably dominated by deposition of natural material on the initially cleaned sites. The average rate of total particulate accumulation on the deposition test sites is 7.03 μg m^{-2} sec^{-1}, which is the same magnitude observed by studies of solid mass accumulation on paved roads (Tomanovic and Maksimovic, 1996) and on Highway (Kim, 2002).

4.8. Metrological data

There was little day-to-day variability in the meteorological data measured during the sampling (Table 6 and Figures 22 and 23), but hour-to-hour variability during daytime period was observed. Mean wind speeds ranged from 0.9 m s^{-1} to 1.3 m s^{-1}, mean temperatures ranged from 11 ºC to 22 ºC, and mean relative humidity ranged from 35 % to 76 %. One of sampling date , 2/8/06, showed extreme values in mean wind speed of 1.9 m s^{-1}, 28 ºC of mean temperature, and 9 % of mean relative humidity. These relatively small ranges for mean wind speed and mean temperature, both of which typically have large diurnal variations, were in part due to the use of 24-hour averages. Wind direction varied hourly.

Pearson correlation analysis indicates high correlation between meteorological conditions only between temperature and the detected mass of rare earth in the resuspension study ($r>0.69$ for Ir, $r>0.33$ for Dy). In both the resuspension and deposition experiments it is likely most of the resuspension occurred immediately after exposure to the wind so that wind speed was not an important factor. Most of cases of strong wind speeds (in the range from 5 m s^{-1} to 9 m s^{-1}) occurred during deployment period early in the day.

5. Conclusions and recommendations

5.1. The NAA analysis method

This study demonstrated that NAA can be used as the basis for an aerosol/particulate tracer

methodology. All aspects of the NAA procedures (labeling, irradiation, counting) worked as planned, including the ability of the method to distinguish between particles labeled with different rare earths in the same sample. Although the per sample cost of irradiation are modest ($10/sample), when the labor in sample preparation and analysis are included the estimated average cost of the sample analysis for resuspension study was $52/sample and the reactor visit and analysis cost for deposition study was $80/sample. These costs are comparable to alternative analytical methods such as ICP-MS.

5.2. Factors affecting tracer detectability

One of the potential advantages of the NAA method is the possibility of detecting small amounts of rare earth mass in samples with low "natural" background levels. In this study the detectability was limited by several factors:

- Variability in analysis results indicated by counting errors and by replicate samples indicates a minimum detectable mass of Dy and Ir on the order of 0.01-0.1 μg, which is several orders of magnitude larger than expected based on literature values. The reasons for this variability are not known precisely, but may have to do in part with gamma emissions from other elements that overlap Dy and Ir emissions.
- Background levels of Dy and Ir in silica, sample vials, and natural deposited material and soils were sufficiently high to limit detection of Dy and Ir, particularly in the deposition study.
- The level of Ir labeling in the silica was lower than reported in the literature.

It is possible that better tracer detection could be obtained using different rare earth elements, such as gold or indium, which may be found to have less overlap with other elements, lower background levels, and higher labeling levels. It is recommended that future studies systematically investigate these aspects of alternative rare earths.

5.3. Tracer deployment and recovery

The methodologies used for tracer deployment and recoveries worked well, but were affected by several issues:

- Although the addition of Arizona Dust greatly reduced the cohesiveness of the silica spheres and improved the handling characteristics of the tracer material, clumping of the tracer material was observed in test area where tracer was deployed. Only a few combinations of Arizona Dust and silica were investigated, leaving the possibility material with different proportions of silica and Arizona Dust might yield significantly better results.
- Experience showed the handling characteristics of the tracer material dictated minimum total surface mass loading of deployed tracer material of about 10 g m^{-2}, which is an order of magnitude greater than observed on natural surfaces (SCAQMD, 1991). It is not known what effect this exaggerated level of mass loading may have had on the observed resuspension and deposition relative to that of natural material.
- The experimental results obtained in this study imply a significant loss of tracer

material immediately after exposure to wind and, possibly, during deployment in spite of multiple wind barriers (boxes and tents). It is not known to what extent this rapid resuspension is typical of natural particulate material in the size range of the tracer particles or how the resuspension potential might be altered if the proportion of Arizona Dust were increased.

- The vacuum recovery system worked basically well, although there is some uncertainty regarding the proportion of tracer material lost in the vacuum system. The experimental results indicate a significant fraction of the deployed tracer remained sequestered on the test surface in spite of vacuuming, but it is not known whether additional material could have been recovered with a more powerful vacuum.

It is recommended future studies investigate systematically the handling characteristics and resuspension potential of alternative tracer materials, possible modifications to the wind barriers used in this study, changes in the vacuum recovery system that would minimize the loss of tracer, and the dependence in tracer sequestration as a function of vacuum design and power.

5.4. Applications of the NAA tracer methodology

The initial hopes for this methodology were that it would provide a cost-effective way to use a tracer that could be detected at very low levels. These expectations were based on reported values of rare earth labeling in porous silica, detection limits on the order of nanograms, and low background concentrations in the natural environment. The results of this study indicate that, at least for the rare earth elements Dy and Ir, the level of labeling is lower than hoped for, the detection limits are 10 to 100 ng, and, most significantly, the background levels in almost all of the materials involved in the methodology (silica, vials, soil, etc.) are sufficiently high that it was impossible to detect deposited tracer that had been diluted in the atmosphere by dispersion.

Unless the issues of modest labeling and high background levels are solved, it appears that the NAA methodology will be useful primarily in studying particle resuspension for which the tracer mass in samples can be manipulated to be above background values. This is achieved simply by initially depositing sufficient mass of tracer. Particle resuspension can potentially be quantified over much larger areas than used in this study and from other types of surfaces such as soil and vegetation. Using the silica labeling levels achieved in this study and assuming a tracer material aerial loading of about 5 g m^{-2}, the cost of the tracer material for a resuspension study would be on the order of $1 per m^2.

It is recommended future studies investigate the use of the NAA tracer methodology to measure particle resuspension from a range of surface types at a scale large enough to provide meaningful information about this important aerosol transport process.

6. References

Baker, J. E. (1997). "Atmospheric Deposition of Contaminants to the Great Lakes and Coastal Waters." Pensacola, FL, SETAC Press.

Bierly, E. W., and G.C.Gill (1963). "A Technique for measuring atmospheric diffusion." Journal of applied meteorology 2: 145-150.

Byrne, M. A. (1995). "An experimental study of the deposition of aerosol on indoor surfaces." Ph.D Thesis in Department of Mechanical Engineering of Imperial College, London.

Byrne, M. A., Goddard, A.J.H., Lange, C. and Roed, J. (1995). "Stable tracer aerosol deposition measurements in a test chamber." J. Aerosol Sci. **26**: 645-653.

Chamberlain, A. C. (1967). "Transport of Lycopodium spores and other small particles to rough surfaces." Proceedings of the Royal Cociety of London series A mathematical and physical sciences **296**(1444): 45-70.

Chow, J. C., Liu, C.S., Cassmassil, J., Watson, J.G., Lu, Z., and L. C. and Pritchett (1992). "A neighborhood scale study of PM10 source contributions in Rubidoux, California." Atmospheric Environment 26A(4): 693-706.

Clough, W.S. (1975). “The deposition of particles on moss and grass surfaces.” Atmospheric Environment 9:1113-1119.

Costrell, L., Unterweger, M.P., and Ahmad, N. (1999). “American National Standard for Calibratin and Use of Germanium Spectrometers for the Measurement of Gamma-Ray Emission Rates of Radionuclides.” The Institute of Electrical and Electronics Engineers, Inc. NY

Datta, S., Mcconnell, L.L., Baker J.E., Lenoir, J and Seiber, J.N (1998). "Evidence for atmospheric transport and deposition of polychlorinated biphenyls to the Lake Tahoe Basin, California-Nevada." Environmental Science and Technology 32: 1378-1385.

Davis, A. P., Shokouhian, M. and Ni Sheubei (2001). "Loading estimates of lead, copper, cadmium, and zinc in urban runoff from specific sources." Chemosphere 44: 997-1009.

Ehmann, W. D. and D. E. Vance (1991). "Radiochemistry and nuclear methods of analysis." Chemical Analysis 116(A wiley-interscience publication, John Wiley& Sons, INC.).

Franz, T. P., Elsenreich, S.J and Holsen, T.M (1998). "Dry deposition of particulate polychlorinated biphenyls and polycyclic aromatic hydrocarbons to Lake Michigan." Environmental Science and Technology 32: 3681-3688.

Garnaud, S., Mouchel, J-M., Chebbo, G. and Thevenot, D.R (1999). "Heavy metal concentrations in dry and wet atmospheric deposits in Paris district: comparison with urban runoff." The Science of the Total Environment 235: 235-245.

Giess, P., A. J. H. Goddard, G. Shaw and D. Allen (1994). "Resuspension of monodisperse particles from short grass swards: A wind tunnel study." Journal of aerosol science 25(5): 843-857.

Gilmore, G. and J. D. Hemingway (1995). "Practical gamma-ray spectrometry." John Wiley & Sons.

Glascock, M.D. (1996). "An overview of neutron activation analysis." http://www.missouri.edu/~glascock/naa_over.htm.

Hay, J.S. and Pasquill, F. (1957). " Diffusion from a fixed source at a height of a few hundred feet in the atmosphere." Journal of Fluid Mechanics 2:299

Houck J.E., Chow J.C., Watson J.G., Simons C.A., Pritchett L.C., Goulet J.M., and Frazier C.A. 1989. Determination of particle size distribution and chemical composition of particulate matter from selected sources in California. Executive summary. Report No. A6-175-35. Prepared for California Air Resources Board, Sacramento, CA, by Desert Research Institute, Reno, NV.

Houck J.E., Goulet J.M., Chow J.C., Watson J.G., and Pritchett L.C. 1990. Chemical characterization of emission sources contributing to light extinction. Pp. 437-446. In: Mathai CV (Ed), Transactions, Visibility and Fine Particles. Air and Waste Management Association, Pittsburgh, PA.

Huber, H. (2003). "Application of g,g-coincidence spectrometry for the determination of iridium in impact related rocks, glasses, and microtektites." *Ph.D. Dissertation*, Institute of Geological Sciences, University of Vienna, Austria.

Jayasekera, P. N., Leese-Weller, R.J., Watterson, J.D., Apsimon, H.M., Bell, J.N.B., Goddard, A.J.H., Minski,M.J., Taylor-Russell, A.J. (1989). "Aerosol containing activatable tracers for wind tunnel studies." Proceeding of 2nd Annual Conference of the Aerosol Society: 107-112.

Kim, L-H (2002). "Monitoring and modeling of pollutant mass in urban runoff: Washoff, buildup and litter." *Ph.D. Dissertation*, University of California, Los Angeles, CA

Lai, A.C.K., Byrne, M.A., and Goddard A.J.H. (2002). "Experimental studies of the effect of rough surfaces and air speed on aerosol deposition in a test chamber." Aerosol Science and Technology 36: 973-982.

Lim, Jeong-Hee (2006). "Atmospheric deposition and resuspension of suspended particulates in an urban area." *Ph.D. Dissertation*, University of California, Los Angeles, CA.

Lim, J-H. , Sabin, L.D., Schiff, K.C., Stolzenbach, K.D. (2006). "Concentration, size distribution, and dry deposition rate of particle-associated metals in the Los Angeles region." Atmospheric Environment 40:7810-7823.

Little, P. (1977). "Deposition of 2.75, 5.0 and 8.5 µm particles to plant and soil surfaces."

Environmental Pollution **12**(4): 293-305.

Lu, R., Turco, R.P., Stolzenbach, K.D., Friedlander, S., Xiong, C., Schiff, K., Tiefenthaler, L (2003). "Dry deposition of airborne trace metals on the Los Angeles Basin and adjacent coastal waters." Journal of Geophysical Research 108(D2): 4074.

Ondov, J. M. (1996). "Particulate tracers for source attribution: potential for application to California's San Joaquin Valley." Journal of Aerosol Science 27(Suppl. 1): s687-s688.

Paerl, H. W. (1995). "Coastal eutrophication in relation to atmospheric nitrogen depositi0n:current perspectives." Ophelia 41: 237-259.

Paode, R. D., Sofuoglu, S.C., Sivadechathep, J., Noll, K.E., Holsen, T.M and Keeler, G.J (1998). "Dry Deposition fluxes and mass size distributions of PB, Cu, and Zn measured in Southern Lake Michigan during AEOLOS." Environmental Science and Technology 32: 1629-1635.

Sabin, L.D., Lim, J-H., Stolzenbach, K.D., Schiff, K.C. (2006a). "Atmospheric dry deposition of tracer metals in the coastal region of Los Angeles, California, USA." Environmental Toxicology and Chemistry 25(9):2334-2341.

Sabin, L.D., Lim, J-H., Venezia, M.T., Winer, A.M., Schiff, K.C., Stolzenbach, K.D (2006b). "The dry deposition and resuspension of particle-associated metals near a freeway in Los Angeles." Atmospheric Environment 40:7528-7538.

Scudlark, J. R., Russell, K.M., Galloway, J.N., Church, T.M. and Keene, W.C (1998). "Organic nitrogen in precipitation at the mid Atlantic US coast-methods evaluation and preliminary measurements." Atmospheric Environment 32: 1719-1728.

Shaw, G., Farrington-Smith, J.G., Kinnersley, R.P. and Minski, M.J. (1994). "Dry deposition of aerosol particles within model spruce canopies." Science of The Total Environment 157(1-3): 17-23

Shemel, G. A. (1973). "Particle resuspension from an asphalt road caused by car and truck traffic." Atmospheric Environment **7**: 291-301.

Simick, M. F., Franz, T.P., Zhang, H., and S. J. Eisenreich (1998). "Gas-particle partitioning of PCBs and PAHs in the Chicago urban and adjacent coastal atmosphere:state of equilibrium." Environmental Science and Technology 32: 251-257.

South Coast Air Quality Management District (1991). "Inventory of PM10 emissions from fugitive dust sources in the South Coast Air Basin." Prepared by South Coast Air Quality Management District, El Monte, CA.

Stolzenbach, K. D., Lu, R., Xiong, C., Friedlander, S., Turco, R., Schiff, K., Tiefenthaler, L (2001). "Measuring and Modeling of Atmospheric Deposition on Santa Monica Bay and the Santa Monica Bay Watershed." Report to the Santa Monica Bay Restoration Project.

Suarez, A. E., P.F. Caffrey., P.V.Borgoul., and J.M.Ondov (1998). "Use of an Ir tracer to determine the size distribution of aerosol emitted from a fleet of diesel sanitation trucks." Environmental Science and Technology 32: 1522-1529.

Tomanovic, A., and Maksimovic, C (1996) “Improved modeling of suspended solids discharge from asphalt surface during storm event” Water Science and Technology, 33: 363-369.

Van Metre, P. C. and B. J. Mahler (2003). "The contribution of particles washed from rooftops to contaminant loading to urban streams." Chemosphere 52: 1727-1741.

Wagenpfeil, F., H.G.Paretzke., J.M.Peres., and J.Tschiersch (1999). "Resuspension of coarse particles in the rgion of Chernobyl." Atmospheric environment 33: 3313-3323.

Watson, J. G., and Chow, J. C. (2000). "Reconciling Urban Fugitive Dust Emissions Inventory and Ambient Source Contribution Estimates: Summary of Current Knowledge and Needed Research." Desert Research Institute DRI Document No. 6110.4F.

Wedepohl, K. H. (1995). "The composition of the continental crust." Geochimica et Cosmochimica Acta **59**: 1217-1232.

Yi, S. M., Shahin., Holsen, T.M and Noll, K.E (1997). "Comparison of dry deposition predicted from models and measured with a water surface sampler." Environmental Science and Technology 31: 272-278.

Yi, S. M., Shahin, U., Sivadechathep, J., Sofuoglu, S.C and Holsen, T.M ((2001). "Overall elemental dry deposition velocities measured around Lake Michigan." Atmospheric Environment 35: 1133-1140.

7. Inventions reported and copyrighted materials produced

None.

8. Glossary of terms, abbreviations, and symbols

ARB	California Air Resources Board
PAH	Polycyclic Aromatic Hydrocarbon
PCB	Polychlorinated biphenyl
NAA	Neutron Activation Analysis
UCLA	University of California, Los Angeles
UCI	University of California, Irvine
Ir	Iridium
Dy	Dysprosium
SV	Sample Vial
HPGe	Hyperpure Germanium
CV	Coefficient of Variation
PVC	Polyvinyl Chloride

Table 1 Mean concentration of rare earth elements in blanks and labeled samples

Blanks or Samples	Ir ($\mu g\ g^{-1}$)			Dy ($\mu g\ g^{-1}$)		
Process silica blank	0.019	±	0.014	0.50	±	0.20
Pure silica blank	0.079	±	0.10	0.076	±	0.029
Soil	0.019	±	0.015	3.6	±	1.4
Arizona Dust	0.025	±	0.030	1.5	±	0.22
Labeled silica	43	±	39	1900	±	410
Crustal value *	0.000050			3.8		

* Wedepohl, 1995

Table 2 Mass of rare earths in blanks

Blanks	Ir (µg)			Dy (µg)		
Filter	0.0028	±	0.0032	0.034	±	0.043
Large sample vial*	0.0059	±	0.00	0.015	±	0.00
Small sample vial	0.00045	±	0.00035	0.0011	±	0.00031
Mylar Sheet	0.0031	±	0.00040	0.0070	±	0.0034

* Large sample vial mass was computed using mass of small sample vial

Table 3 Concentration (μg g^{-1}) and mass (μg) of rare earth elements in background samples

Experiment	Test #	Test Date	Collected total mass (g)	Concentration (μg g^{-1})		Detected Mass (μg)		Area Normalized Depositon (μg m^{-2})	
				Dy	Ir	Dy	Ir	Dy	Ir
Resuspension	1	1/9/2006	0.607	ND	0.00474	ND	0.00243	ND	0.0749
Resuspension	2	1/9/2006	1.19	ND	0.0196	ND	0.0229	ND	0.706
Resuspension	3	2/8/2006	0.292	2.22	0.00555	0.648	0.00118	20.0	0.0364
Resuspension	4	2/8/2006	0.285	1.59	0.00452	0.454	0.000844	14.0	0.0260
Resuspension	5	3/14/2006	0.609	1.41	0.000631	0.859	ND	26.5	ND
Resuspension	6	3/14/2006		1.15	0.00405	0.700	0.00202	21.6	0.0623
Deposition	1	4/6/2006	0.227	0.937	0.000216	0.198	ND	6.11	ND
Deposition	2	4/6/2006	0.0992	3.17	0.00256	0.299	ND	9.22	ND
Deposition	3	5/1/2006	0.278	2.63	0.000649	0.678	ND	20.9	ND
Deposition	4	5/17/2006	0.328	3.41	0.00593	1.06	0.000356	32.7	0.0110

ND: Non-detect sample

Table 4 Masses and recovery percentages for resuspension experiment

Test #	Time (days)	Total mass (g)			Dy (µg)			Ir (µg)		
		Deployed	Collected	Recovery (%)	Initially deployed	Detected mass	Recovery (%)	Initially deployed	Detected mass	Recovery (%)
1	0	0.248	0.0939	37.8	121	54.8	45.3	2.49	1.25	50.0
1	0.25	0.250	0.0641	25.6	117	28.5	24.3	2.67	0.570	21.4
1	1	0.257	0.0484	18.8	118	21.3	18.1	2.59	0.510	19.7
1	2	0.243	0.0521	21.4	115	14.0	12.1	2.72	0.786	28.9
1	3	0.255	0.0710	27.9	116	32.9	28.4	2.81	0.802	28.6
1	4	0.250	0.0403	16.1	124	22.8	18.4	2.47	0.441	17.9
2	0	0.247	0.0738	29.9	120	28.8	24.1	2.66	0.993	37.3
2	0.25	0.253	0.0629	24.9	120	19.7	16.4	2.92	0.542	18.6
2	1	0.243	0.0488	20.1	119	26.9	22.6	2.57	0.548	21.3
2	2	0.246	0.0615	25.0	123	27.8	22.6	2.44	0.606	24.8
2	3	0.250	0.0403	16.2	120	12.9	10.8	2.70	0.386	14.3
2	4	0.248	0.0763	30.8	122	17.5	14.3	2.50	0.768	30.7
SC1	4	0.249	0.150	60.4	121	15.0	12.4	2.55	1.61	62.9
3	0	NS	NS	NS	NS	NS	NS	NS	NS	NS
3	0.083	0.350	0.0729	20.8	247	24.4	9.87	11.2	0.982	8.73
3	0.167	0.306	0.0846	27.7	253	28.9	11.4	11.5	1.97	17.2
3	0.25	0.326	0.131	40.1	254	51.2	20.1	13.1	3.97	30.4
3	0.333	0.301	0.0736	24.5	239	39.0	16.3	12.0	1.91	15.9
4	0	0.271	0.172	63.7	210	66.6	31.8	11.0	8.50	77.0
4	0.083	0.280	0.134	47.8	212	63.6	30.0	10.5	4.09	38.8
4	0.167	0.288	0.186	64.6	210	67.5	32.1	12.1	8.53	70.7
4	0.25	0.271	0.152	56.0	211	52.6	25.0	10.7	6.55	61.3
4	0.333	0.273	0.0932	34.2	215	40.5	18.8	10.3	3.04	29.4
SC2	0.333	0.301	0.219	72.5	235	45.2	19.2	11.6	10.5	90.3
5	0	0.302	0.220	73.0	162	69.7	43.0	1.14	0.914	80.4
5	0.083	0.287	0.136	47.2	142	42.8	30.0	1.16	0.603	51.9
5	0.167	0.283	0.164	57.8	151	62.2	41.3	1.12	0.542	48.2
5	0.333	0.300	0.116	38.7	162	42.0	25.9	1.22	0.463	37.9
5	1	0.299	0.111	37.0	162	27.0	16.7	1.21	0.339	28.1
5	2	0.300	0.148	49.1	165	40.6	24.6	1.20	0.542	45.0
6	0	0.290	0.219	75.5	155	73.4	47.5	1.16	0.874	75.7
6	0.083	0.297	0.0561	18.9	162	10.2	6.3	1.17	0.258	22.0
6	0.167	0.302	0.134	44.6	161	44.0	27.3	1.21	0.442	36.4
6	0.333	0.295	0.139	47.1	162	43.7	27.1	1.19	0.529	44.3
6	1	0.297	0.149	50.2	158	42.8	27.1	1.22	0.430	35.2
6	2	0.310	0.161	51.9	164	42.4	25.8	1.21	0.556	45.8
SC3	2	0.302	0.169	55.8	163	82.5	50.6	1.23	0.589	47.9

SC: Surface Control- SC1 for test 1 and 2; SC2 for test 3 and 4; SC3 for test 5 and 6
NS: Not Sampled

Table 5 Masses and recoveries for deposition experiment

Test #	Location	Total mass(g)			Dy					Area Normalization (μg m^{-2})		Ir					Area Normalization (μg m^{-2})	
		Deployed	Collected	Recovery(%)	Initially deployed (μg)	Detected mass(μg)	Recovery (%)	Deposition Plate (μg)	Asphalt Surface (μg)	Deposition Plate	Asphalt Surface	Initially deployed (μg)	Detected mass(μg)	Recovery (%)	Deposition Plate(μg)	Asphalt Surface (μg)	Deposition Plate	Asphalt Surface
1	M	1.75	1.43	81.6	1390	567	40.7					13.2	13.8	104.7				
1	1	0.00	0.00420					0.0123	ND	1.23	ND				0.0171	ND	1.71	ND
1	2	0.00	0.0178					ND	0.0801	ND	2.47				ND	ND	ND	ND
1	3	0.00	0.00860					ND	0.0348	ND	1.07				ND	ND	ND	ND
1	4	0.00	0.0335					ND	0.0838	ND	2.58				ND	ND	ND	ND
1	5	0.00	0.0150					ND	0.0365	ND	1.13				ND	ND	ND	ND
1	6	0.00	0.0224					ND	0.0416	ND	1.28				ND	ND	ND	ND
2	M	1.80	1.49	83.1	1450	577	39.8				ND	13.4	14.9	111.6				
2	1	0.00	0.00440					ND	ND	ND	ND				0.0297	ND	0.000	ND
2	2	0.00	0.00960					ND	0.0183	ND	0.563				ND	ND	ND	ND
2	3	0.00	0.00650					0.0171	0.00129	1.71	0.0396				ND	ND	ND	ND
2	4	0.00	0.00470					0.0107	0.0105	1.07	0.323				ND	ND	ND	ND
2	5	0.00	0.0136					ND	0.0265	ND	0.816				0.00180	ND	0.180	ND
2	6	0.00	0.0214					ND	0.0375	ND	1.16				ND	ND	ND	ND
3	M	0.507	0.292	57.6	330	133	40.3					5.54	2.90	52.3				
3	1	0.00	0.00610					ND	ND	ND	ND				ND	ND	ND	ND
3	2	0.00	0.0310					ND	0.147	ND	4.55				ND	ND	ND	ND
3	3	0.00	0.0339					ND	0.0939	ND	2.89				ND	ND	ND	ND
3	4	0.00	0.0466					ND	0.171	ND	5.26				ND	0.0241	ND	0.743
3	5	0.00	0.0506					ND	0.0774	ND	2.39				ND	0.0157	ND	0.485
3	6	0.00	0.0732					ND	0.310	ND	9.56				ND	0.0406	ND	1.25
4	M	1.70	0.800	47.1	1110	580	52.3					18.6	8.47	45.5				
4	1	0.00	0.00490					0.00338	ND	0.338	ND				ND	ND	ND	ND
4	2	0.00	0.0170					0.00482	0.00205	0.482	0.0631				ND	ND	ND	ND
4	3	0.00	0.00900					0.00753	0.0121	0.753	0.373				ND	ND	ND	ND
4	4	0.00	0.0155					0.00117	0.00521	0.117	0.161				ND	ND	ND	ND
4	5	0.00	0.00800					ND	ND	ND	ND				ND	ND	ND	ND
4	6	0.00	0.0155					0.0111	ND	1.11	ND				ND	ND	ND	ND

ND: Non-detect sample
M: Mixture deployed at the center of the sampling location

Table 6 Summary of meteorological data for resuspension experiment

Test #	Time (day)	Temp (˚ C)	Humidity(%)	Wind Dir.(degree)	Wind Speed(m sec^{-1})	Wind Speed max(m sec^{-1})
1	0	22.8	23	160	0.9	1.8
1	0.25	22.3	21.1	306	3.8	6.6
1	1	13.6	37.8	253	1.2	2.7
1	2	13.9	36.2	192	1.2	2.6
1	3	13.8	41.8	155	1.2	2.5
1	4	14.1	42.7	138	1.2	2.5
2	0	23.3	22	320	3.6	8
2	0.25	21.4	22.4	314	3.7	6.3
2	1	13.6	37.7	250	1.2	2.6
2	2	13.9	36.2	170	1.2	2.6
2	3	13.7	42	154	1.2	2.5
2	4	14.1	42.8	137	1.2	2.5
3	0.083	27.7	8.3	65	2.3	5.3
3	0.167	28.7	8.8	118	1.9	4.4
3	0.25	28.7	8.7	137	1.7	4
3	0.333	28.3	8.8	110	1.9	4.6
4	0	27.2	8	60	3	4.9
4	0.083	28.5	8.6	104	2	4.7
4	0.167	29	8.8	133	1.7	4
4	0.25	28.9	8.8	136	1.7	4.1
4	0.333	28.2	8.8	109	1.9	4.6
5	0	16.1	43	210	1.3	3.6
5	0.083	16.5	38.5	200	1.5	3.8
5	0.167	17.6	35.2	197	1.6	4.1
5	0.333	17	37.8	188	2.1	4.5
5	1	11.5	65.1	179	1.3	3.1
5	2	11.2	64.5	150	1.1	2.7
6	0	16.1	37	210	1.3	4
6	0.083	17.6	34.6	193	1.5	3.7
6	0.167	18.1	33.8	187	1.7	4.2
6	0.333	16.7	40.5	189	2.7	4.5
6	1	11.5	64.8	178	1.3	3
6	2	11.2	64.3	150	1.1	2.7

Table 7 Summary of meteorological data for deposition experiment

Test #	Time(day)	Temp (° C)	Humidity (%)	Wind Dir.(degree)	Wind Speed (m sec^{-1})	Wind Speed max(m sec^{-1})
1 &2	1	12.7	71.8	164	1.0	2.5
3	1	18.6	76.4	238	1.2	2.7
4	1	21.9	70.0	272	1.3	2.8

Figure 1 Location of experimental sampling site

Figure 2 View of sampling site

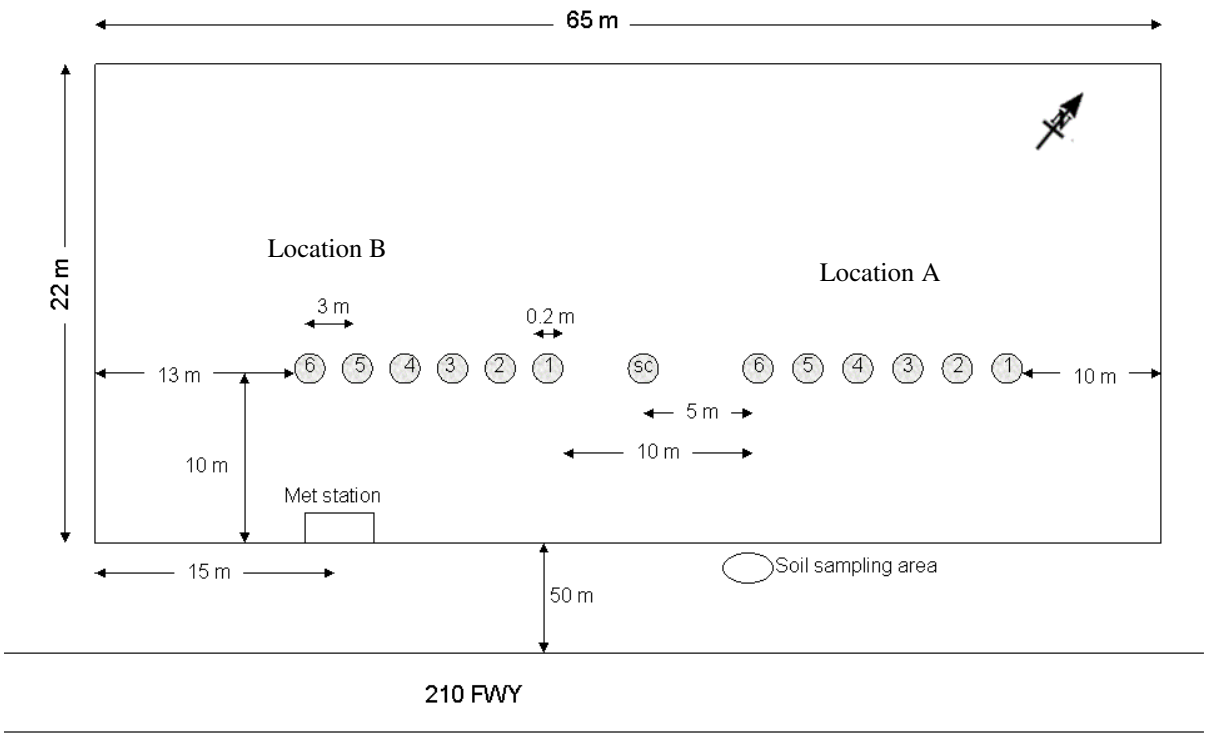

Figure 3 Site layout for resuspension experiment (location A for test 1,3, and 5; location B for test 2,4, and 6); location SC for surface control

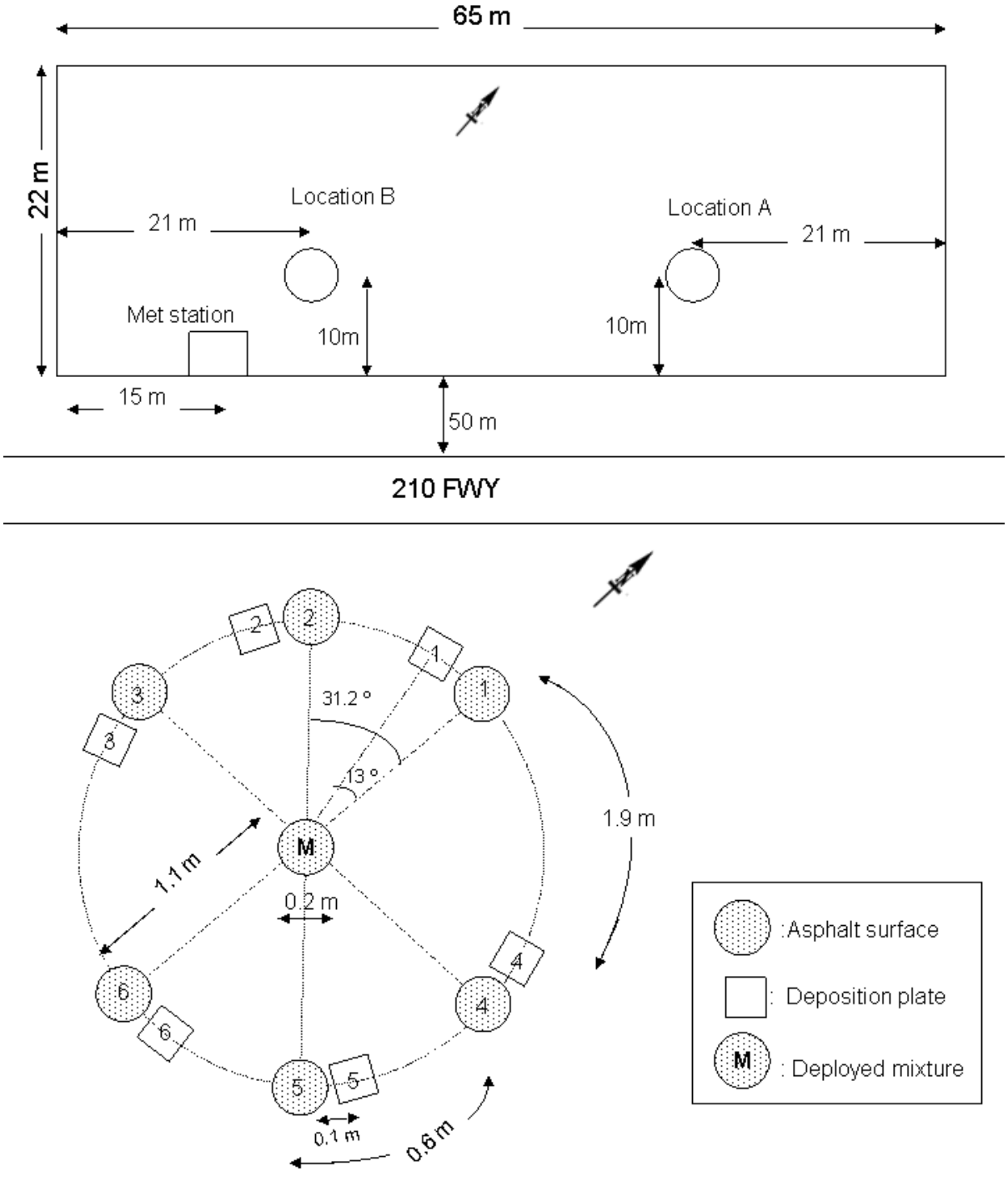

Figure 4 Site layout for deposition experiment (location A for test 1, location B for test 2,3, and 4; lower figure shows detail of sample deployment)

(a)

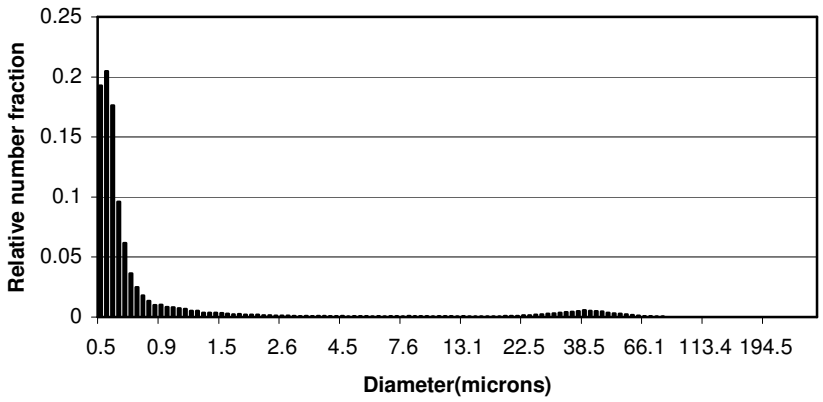

(b)

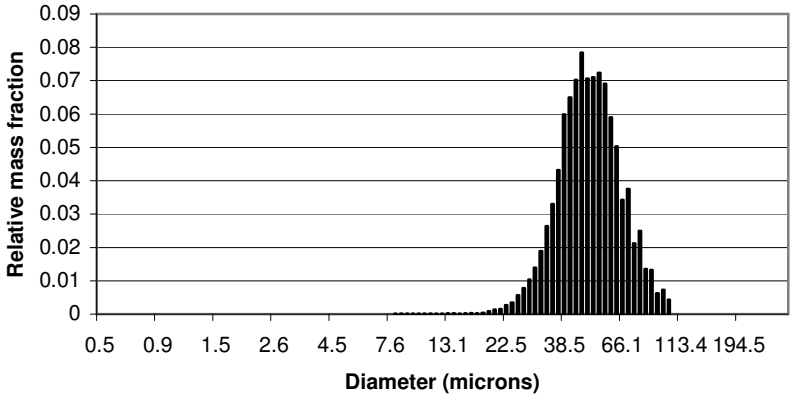

Figure 5 Counts (a) and mass distribution (b) of large silica particles (decantation procedure not applied to these particles)

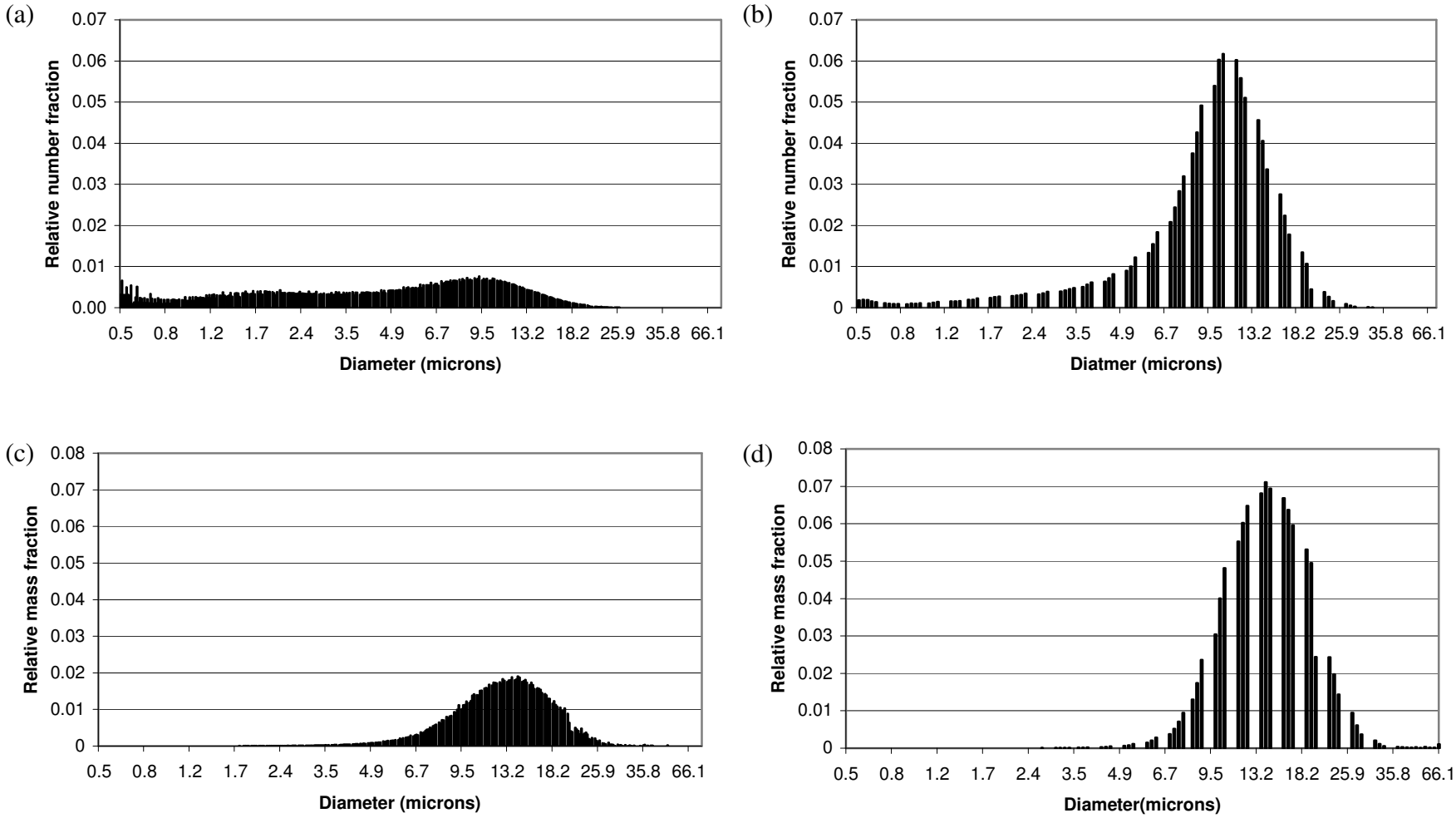

Figure 6 Counts of small particles before (a) and after decanting (b); mass distribution of small particles before (c) and after decanting (d)

Figure 7 Close-up of deployment

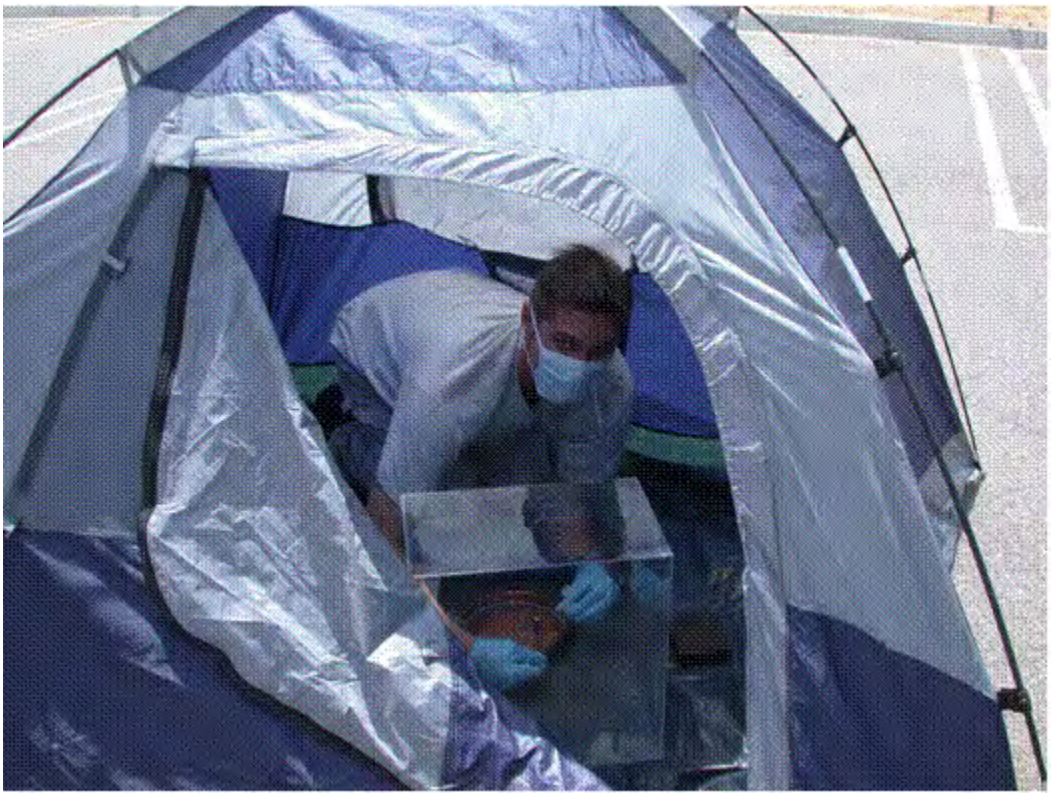

Figure 8 Deployment in a tent

(a)

(b)

Figure 9 Views of layouts for resuspension (a) and deposition (b) experiments

(a)

(b)

(c)

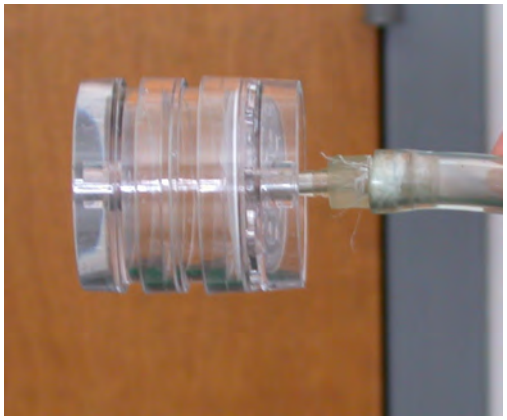

Figure 10 Views of inlet of vacuum recovery system: front (a and b); side (c)

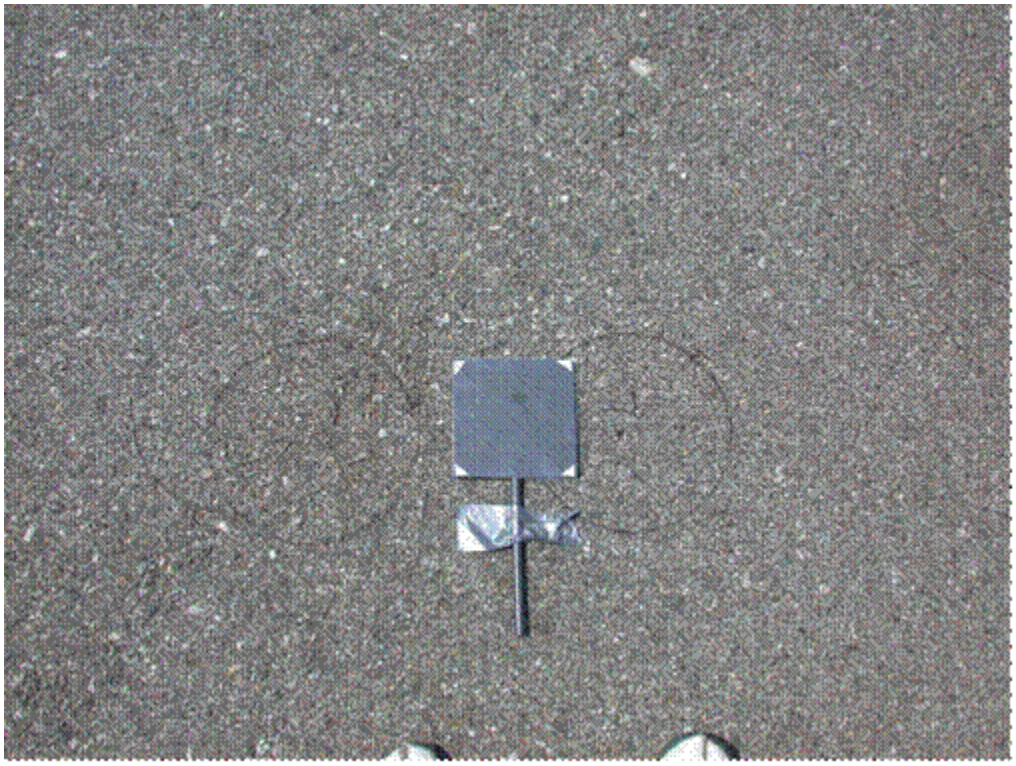

Figure 11 View of deposition plate

Figure 12 View of sample vials

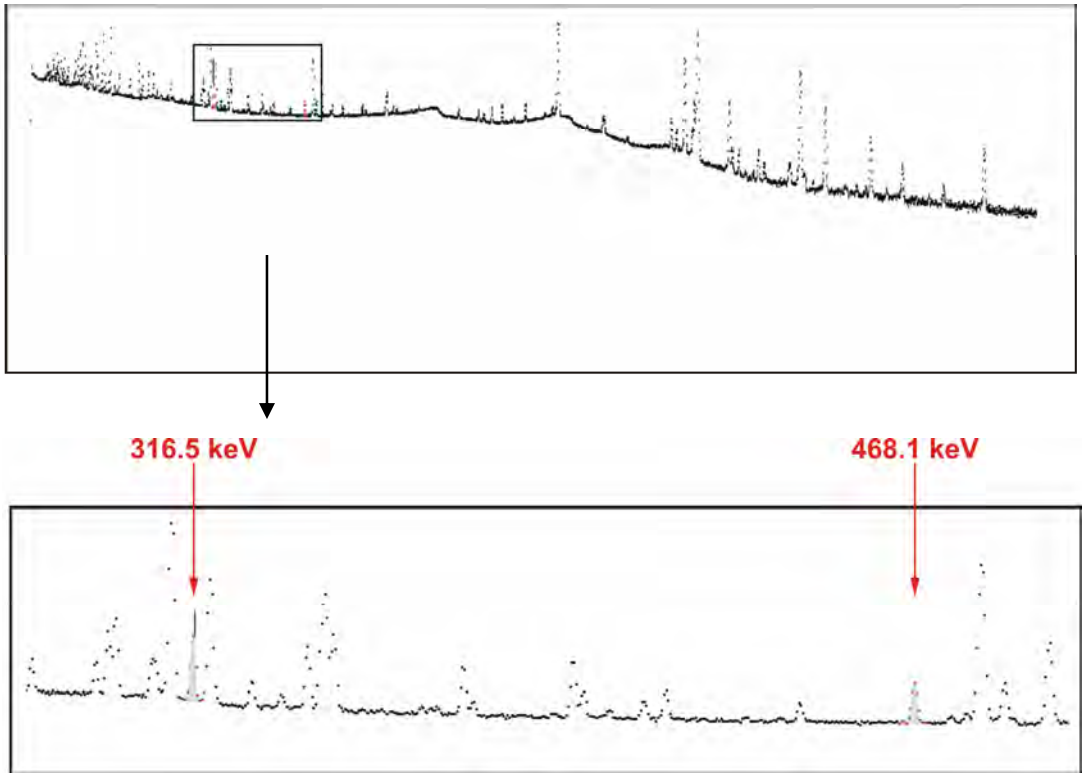

Figure 13 Gamma ray spectrum from 300 to 500 keV showing several elements with two iridium peaks at the energy level of 316.5 and 468.1 keV in soil sample for 3hours of irradiation, decayed for 21days, and counted for 24hours on HPGe detector.

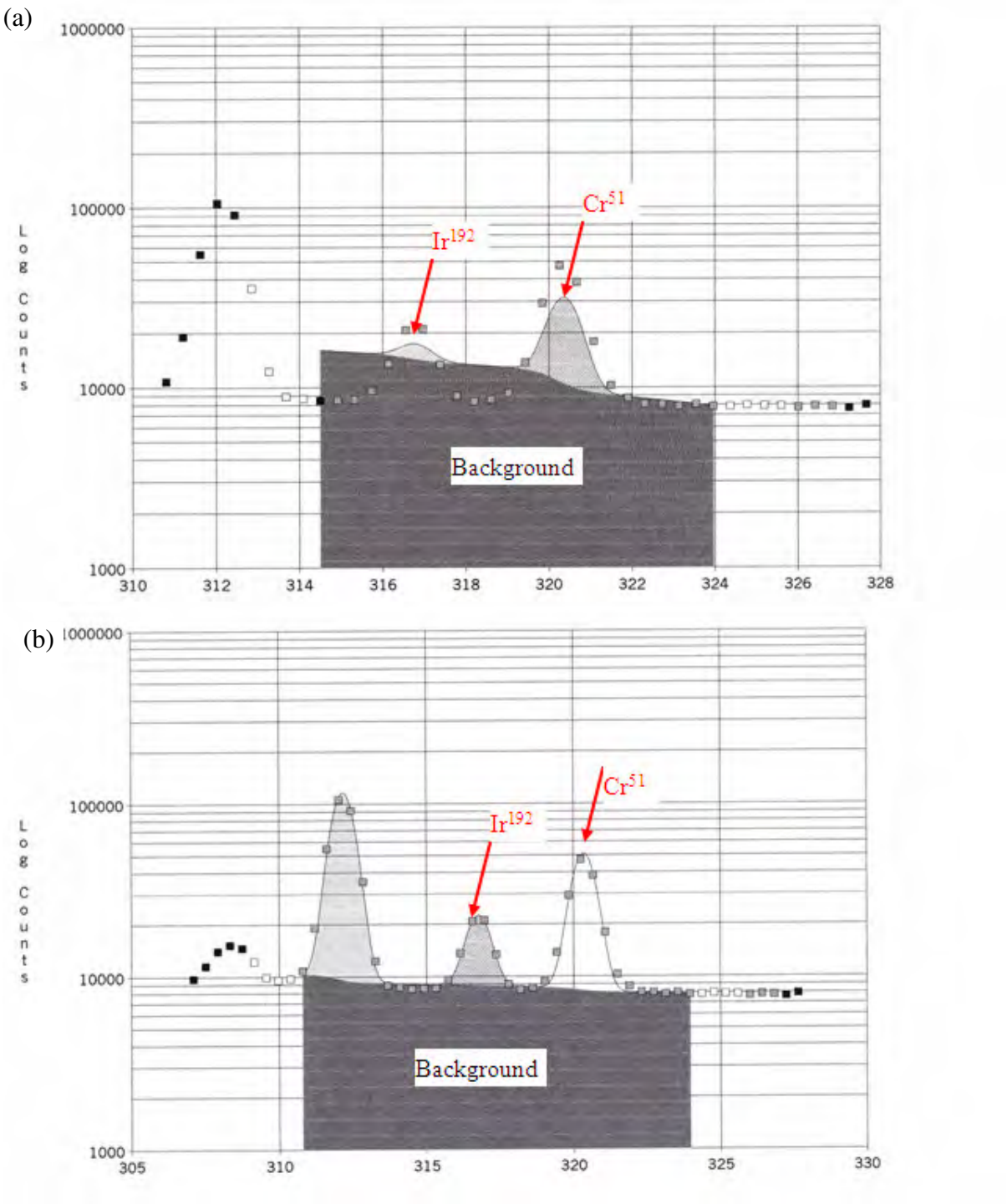

Figure 14 Interference of the Cr^{51} to Ir ^{192} at the energy level of 316 keV and an illustration of gamma peaks for before (a) and after (b) manual adjustment.

Figure 15 View of meteorological station

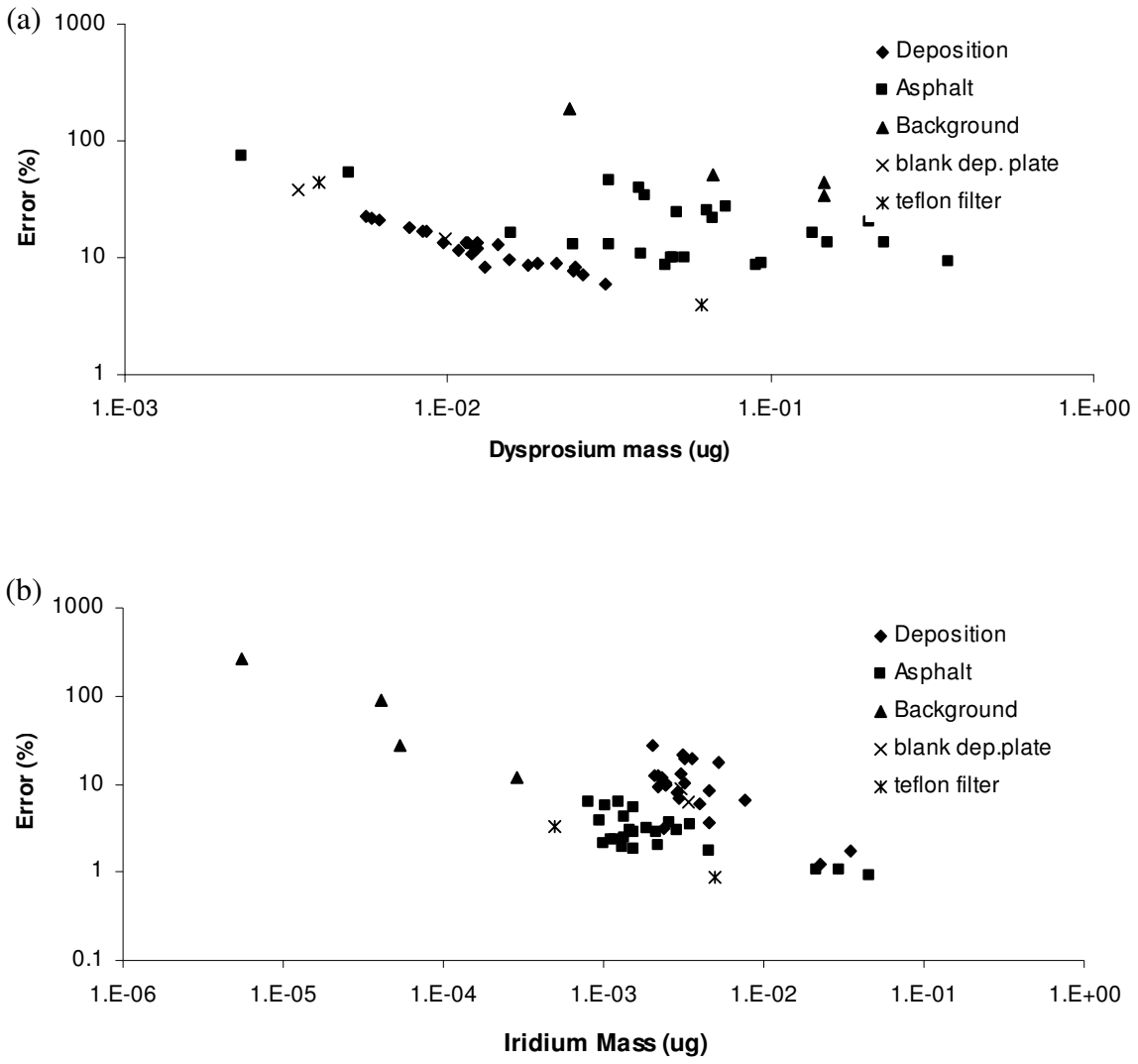

Figure 16 Relative counting error as a function of detected rare earth mass: Dy (a); Ir (b) counting errors

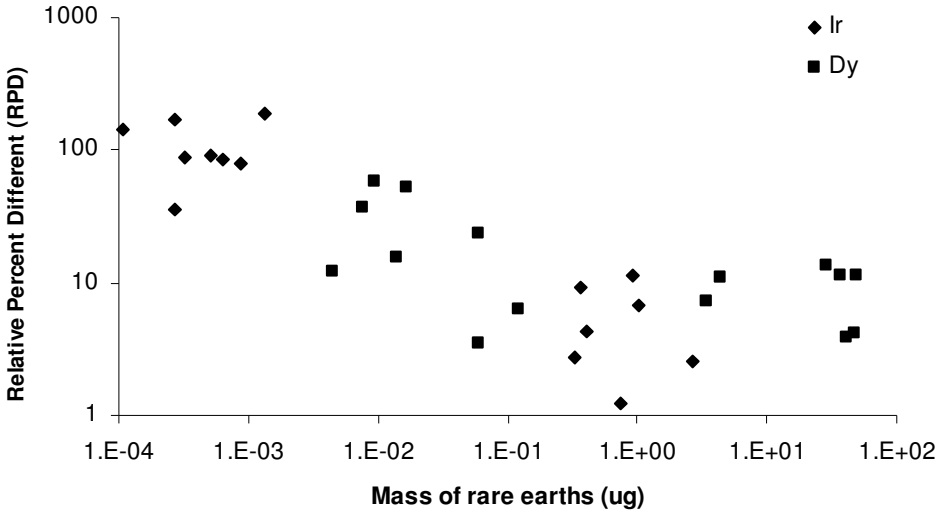

Figure 17 Relative differences between replicates as a function of detected rare earth mass

Figure18 Deployed tracer mixture on the asphalt surface showing particle agglomeration

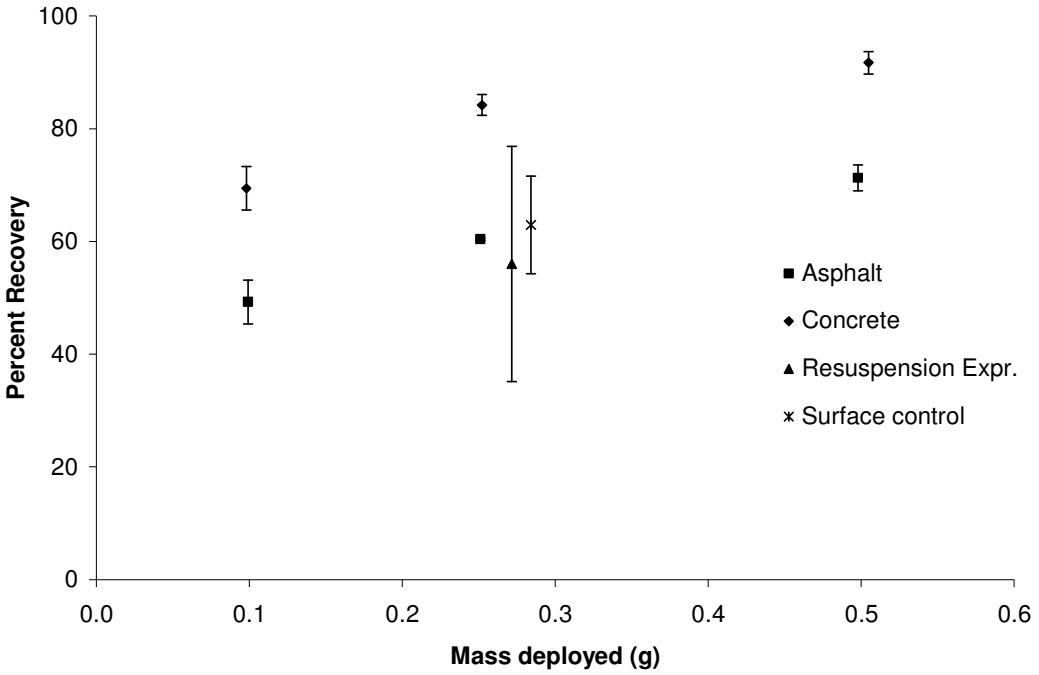

Figure 19 Percent recovery of total particle mass as a function of total particle mass deployed for preliminary experiments on two different surfaces and for the resuspension experiment

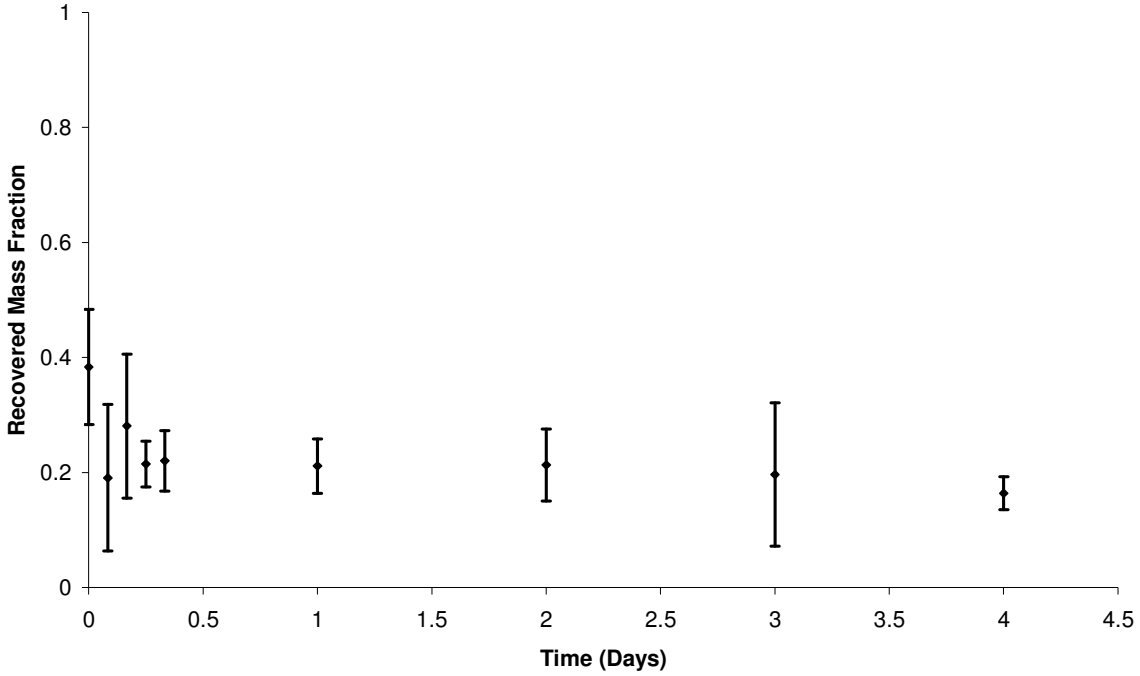

Figure 20 Recovered mass fraction of Dy as a function of time in resuspension experiment

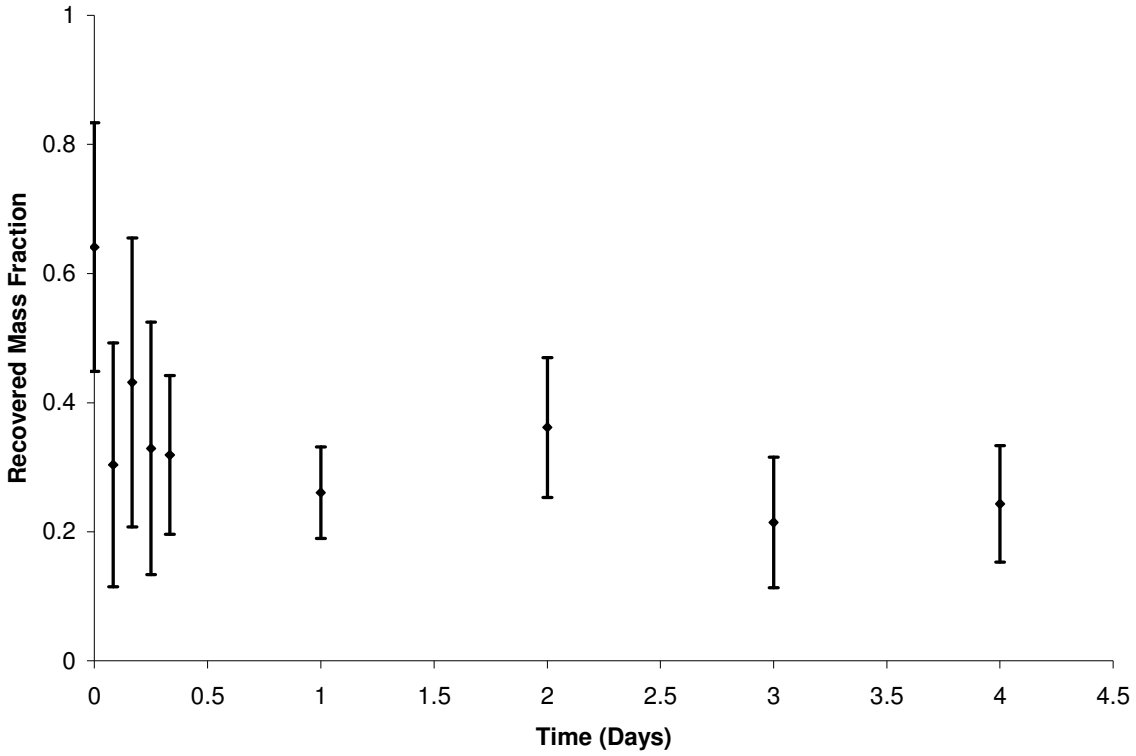

Figure 21 Recovered mass fraction of Ir as a function of time in resuspension experiment

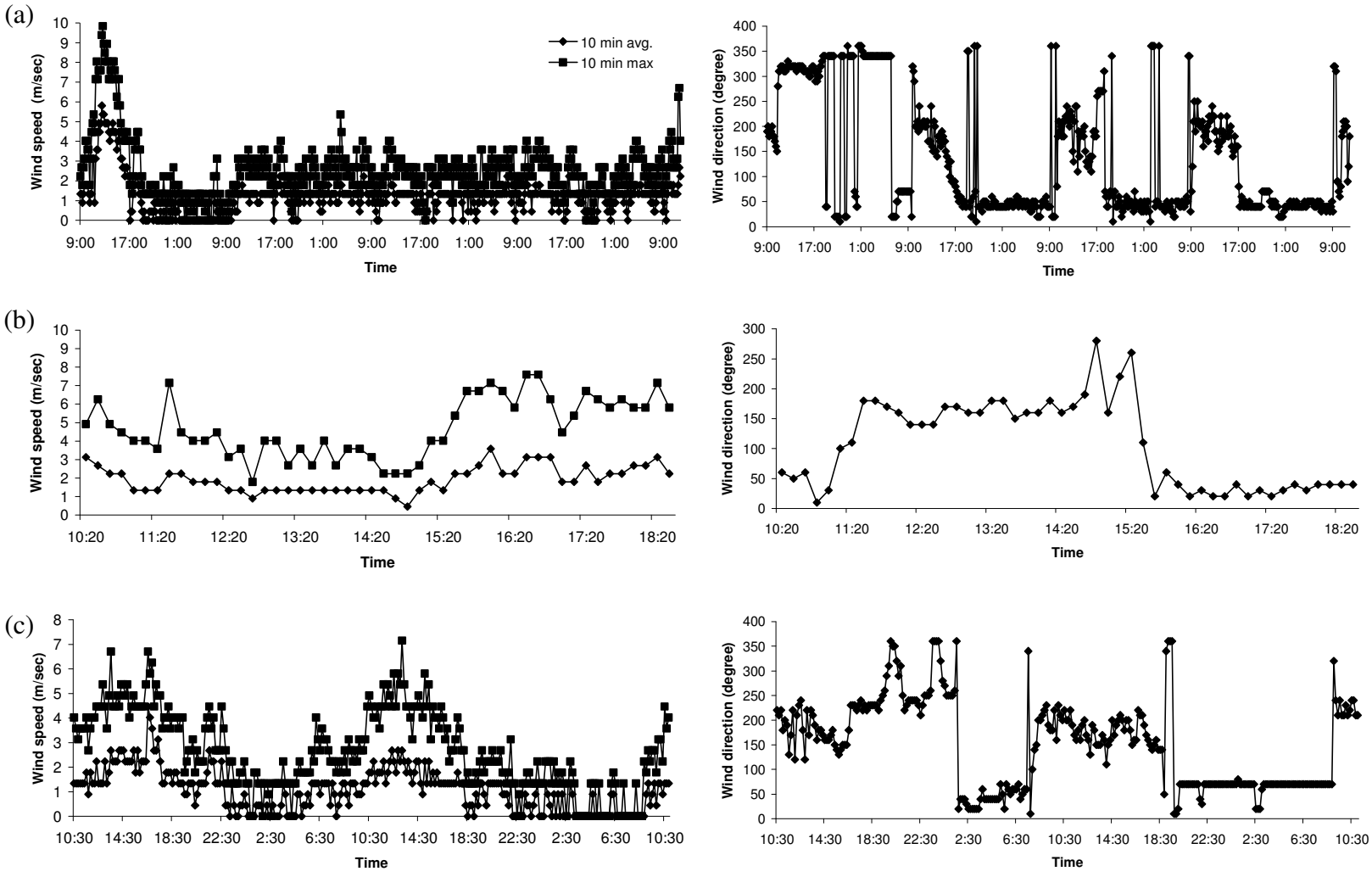

Figure 22 Wind speed and direction during the resuspension experiments: (a) first and second tests; (b) third and fourth tests; (c) fifth and sixth tests

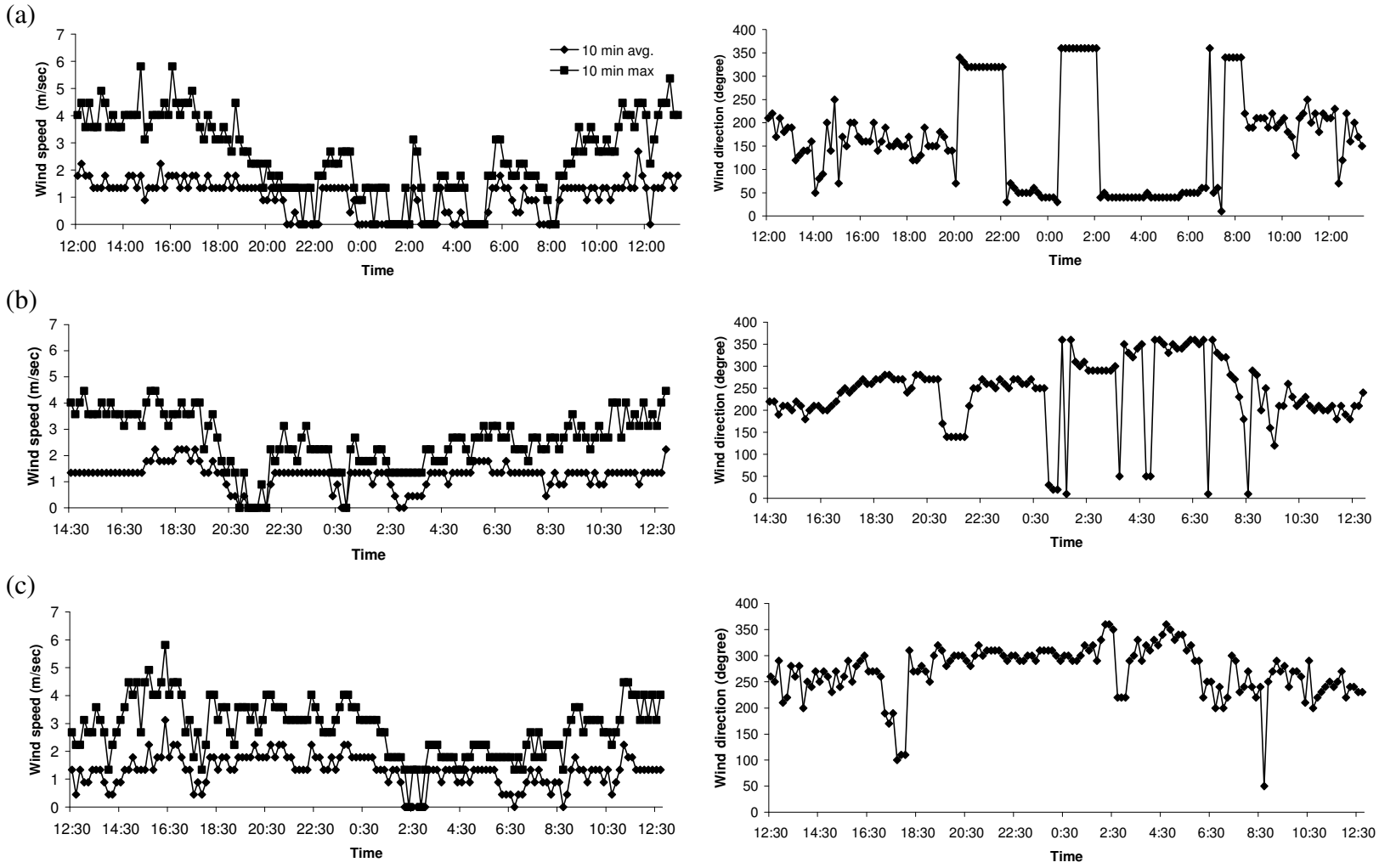

Figure 23 Wind speed and direction during the deposition experiments: (a) first and second tests; (b) third test; (c) fourth test

Appendix A: Database

Table A-1 Key to sample identification number

Experiment Type		Collection Method		Experiment Number	Sampling Site Number	Parameter(Symbol)		Rare Earth Analyzed	
Resuspension study	1	Silica deployed surface	1	1	1	Arizona Dust (AD)	01	Dysprosium	1
DepositIon study	2	Deposition plate	2	2	2	Background (BK)	02	Iridium	2
		Asphalt collection	3	3	3	Dysprosium (Dy)	03		
		Labeling	4	4	4	Dysprosium labeled (DL)	04		
		Met data	5	5	5	Dysprosium standard (SD)	05		
				6	6	Dysprosium standard for larger vial (STD)	06		
						Filter blank (TF)	07		
						Iridium (Ir)	08		
						Iridium labeled (IL)	09		
						Iridium standard (SI)	10		
						Iridium standard for larger vial (STI)	11		
						Mixture (M)	12		
						Mylar blank (BLK)	13		
						Process blank (PB)	14		
						Pure silica blank (P)	15		
						Sample vial large (BV)	16		
						Sample vial small (B)	17		
						Soil (SO)	18		
						Surface control (SC)	19		

Example

ID:1121011= Task 1, Silica deployed surface, 2nd experiment at the first sampling site; Arizona dust was tested to measure Dy mass.

Table A-2 Basic Information

Sample ID	Sample method	Sampling periods	Sampling start	Sampling time(days)	Note
1111	Silica deployed surface	1/9/06 ~ 1/13/06	1/9/06 10:30 AM	0	Resuspension study
1112	Silica deployed surface	1/9/06 ~ 1/13/06	1/9/06 10:30 AM	0.25	Resuspension study
1113	Silica deployed surface	1/9/06 ~ 1/13/06	1/9/06 10:30 AM	1	Resuspension study
1114	Silica deployed surface	1/9/06 ~ 1/13/06	1/9/06 10:30 AM	2	Resuspension study
1115	Silica deployed surface	1/9/06 ~ 1/13/06	1/9/06 10:30 AM	3	Resuspension study
1116	Silica deployed surface	1/9/06 ~ 1/13/06	1/9/06 10:30 AM	4	Resuspension study
1121	Silica deployed surface	1/9/06 ~ 1/13/06	1/9/06 11:40 AM	0	Resuspension study
1122	Silica deployed surface	1/9/06 ~ 1/13/06	1/9/06 11:40 AM	0.25	Resuspension study
1123	Silica deployed surface	1/9/06 ~ 1/13/06	1/9/06 11:40 AM	1	Resuspension study
1124	Silica deployed surface	1/9/06 ~ 1/13/06	1/9/06 11:40 AM	2	Resuspension study
1125	Silica deployed surface	1/9/06 ~ 1/13/06	1/9/06 11:40 AM	3	Resuspension study
1126	Silica deployed surface	1/9/06 ~ 1/13/06	1/9/06 11:40 AM	4	Resuspension study
1131	Silica deployed surface	2/8/2006	2/8/06 9:30 AM	0	Resuspension study
1132	Silica deployed surface	2/8/2006	2/8/06 9:30 AM	0.083	Resuspension study
1133	Silica deployed surface	2/8/2006	2/8/06 9:30 AM	0.167	Resuspension study
1134	Silica deployed surface	2/8/2006	2/8/06 9:30 AM	0.25	Resuspension study
1135	Silica deployed surface	2/8/2006	2/8/06 9:30 AM	0.333	Resuspension study
1141	Silica deployed surface	2/8/2006	2/8/06 10:20 AM	0	Resuspension study
1142	Silica deployed surface	2/8/2006	2/8/06 10:20 AM	0.083	Resuspension study
1143	Silica deployed surface	2/8/2006	2/8/06 10:20 AM	0.167	Resuspension study
1144	Silica deployed surface	2/8/2006	2/8/06 10:20 AM	0.25	Resuspension study
1145	Silica deployed surface	2/8/2006	2/8/06 10:20 AM	0.333	Resuspension study
1151	Silica deployed surface	3/14/06 ~ 3/16/06	3/14/06 9:30 AM	0	Resuspension study
1152	Silica deployed surface	3/14/06 ~ 3/16/06	3/14/06 9:30 AM	0.083	Resuspension study
1153	Silica deployed surface	3/14/06 ~ 3/16/06	3/14/06 9:30 AM	0.167	Resuspension study
1154	Silica deployed surface	3/14/06 ~ 3/16/06	3/14/06 9:30 AM	0.333	Resuspension study
1155	Silica deployed surface	3/14/06 ~ 3/16/06	3/14/06 9:30 AM	1	Resuspension study
1156	Silica deployed surface	3/14/06 ~ 3/16/06	3/14/06 9:30 AM	2	Resuspension study
1161	Silica deployed surface	3/14/06 ~ 3/16/06	3/14/06 10:30 AM	0	Resuspension study
1162	Silica deployed surface	3/14/06 ~ 3/16/06	3/14/06 10:30 AM	0.083	Resuspension study
1163	Silica deployed surface	3/14/06 ~ 3/16/06	3/14/06 10:30 AM	0.167	Resuspension study
1164	Silica deployed surface	3/14/06 ~ 3/16/06	3/14/06 10:30 AM	0.333	Resuspension study
1165	Silica deployed surface	3/14/06 ~ 3/16/06	3/14/06 10:30 AM	1	Resuspension study
1166	Silica deployed surface	3/14/06 ~ 3/16/06	3/14/06 10:30 AM	2	Resuspension study
1311	Asphalt collection	1/9/06 ~ 1/13/06			Background blank
1331	Asphalt collection	2/8/2006			Background blank
1351	Asphalt collection	3/14/06 ~ 3/16/06			Background blank
1411	Labeling	1/4/06 ~ 1/6/06			Labeled silica used for 1/9/06 field test
1412	Labeling	1/30/06 ~ 2/1/06			Labeled silica used for 2/8/06 field test
1413	Labeling	3/7/06 ~ 3/9/06			Labeled silica used for3/14/06 field test
2211	Deposition plate	4/6/06 ~ 4/7/06	4/6/06 12:30 PM	1	Deposition study
2212	Deposition plate	4/6/06 ~ 4/7/06	4/6/06 12:30 PM	1	Deposition study
2213	Deposition plate	4/6/06 ~ 4/7/06	4/6/06 12:30 PM	1	Deposition study
2214	Deposition plate	4/6/06 ~ 4/7/06	4/6/06 12:30 PM	1	Deposition study
2215	Deposition plate	4/6/06 ~ 4/7/06	4/6/06 12:30 PM	1	Deposition study
2216	Deposition plate	4/6/06 ~ 4/7/06	4/6/06 12:30 PM	1	Deposition study
2221	Deposition plate	4/6/06 ~ 4/7/06	4/6/06 1:10 PM	1	Deposition study
2222	Deposition plate	4/6/06 ~ 4/7/06	4/6/06 1:10 PM	1	Deposition study
2223	Deposition plate	4/6/06 ~ 4/7/06	4/6/06 1:10 PM	1	Deposition study
2224	Deposition plate	4/6/06 ~ 4/7/06	4/6/06 1:10 PM	1	Deposition study
2225	Deposition plate	4/6/06 ~ 4/7/06	4/6/06 1:10 PM	1	Deposition study
2226	Deposition plate	4/6/06 ~ 4/7/06	4/6/06 1:10 PM	1	Deposition study
2231	Deposition plate	5/1/06 ~ 5/2/06	5/1/06 12:20 PM	1	Deposition study
2232	Deposition plate	5/1/06 ~ 5/2/06	5/1/06 12:20 PM	1	Deposition study
2233	Deposition plate	5/1/06 ~ 5/2/06	5/1/06 12:20 PM	1	Deposition study
2234	Deposition plate	5/1/06 ~ 5/2/06	5/1/06 12:20 PM	1	Deposition study
2235	Deposition plate	5/1/06 ~ 5/2/06	5/1/06 12:20 PM	1	Deposition study
2236	Deposition plate	5/1/06 ~ 5/2/06	5/1/06 12:20 PM	1	Deposition study
2241	Deposition plate	5/17/06 ~ 5/18/06	5/17/06 12:10 PM	1	Deposition study
2242	Deposition plate	5/17/06 ~ 5/18/06	5/17/06 12:10 PM	1	Deposition study
2243	Deposition plate	5/17/06 ~ 5/18/06	5/17/06 12:10 PM	1	Deposition study
2244	Deposition plate	5/17/06 ~ 5/18/06	5/17/06 12:10 PM	1	Deposition study
2245	Deposition plate	5/17/06 ~ 5/18/06	5/17/06 12:10 PM	1	Deposition study
2246	Deposition plate	5/17/06 ~ 5/18/06	5/17/06 12:10 PM	1	Deposition study
2311	Asphalt collection	4/6/06 ~ 4/7/06	4/6/06 12:30 PM	1	Deposition study
2312	Asphalt collection	4/6/06 ~ 4/7/06	4/6/06 12:30 PM	1	Deposition study
2313	Asphalt collection	4/6/06 ~ 4/7/06	4/6/06 12:30 PM	1	Deposition study
2314	Asphalt collection	4/6/06 ~ 4/7/06	4/6/06 12:30 PM	1	Deposition study
2315	Asphalt collection	4/6/06 ~ 4/7/06	4/6/06 12:30 PM	1	Deposition study
2316	Asphalt collection	4/6/06 ~ 4/7/06	4/6/06 12:30 PM	1	Deposition study
2321	Asphalt collection	4/6/06 ~ 4/7/06	4/6/06 1:10 PM	1	Deposition study
2322	Asphalt collection	4/6/06 ~ 4/7/06	4/6/06 1:10 PM	1	Deposition study
2323	Asphalt collection	4/6/06 ~ 4/7/06	4/6/06 1:10 PM	1	Deposition study
2324	Asphalt collection	4/6/06 ~ 4/7/06	4/6/06 1:10 PM	1	Deposition study
2325	Asphalt collection	4/6/06 ~ 4/7/06	4/6/06 1:10 PM	1	Deposition study
2326	Asphalt collection	4/6/06 ~ 4/7/06	4/6/06 1:10 PM	1	Deposition study
2331	Asphalt collection	5/1/06 ~ 5/2/06	5/1/06 12:20 PM	1	Deposition study
2332	Asphalt collection	5/1/06 ~ 5/2/06	5/1/06 12:20 PM	1	Deposition study
2333	Asphalt collection	5/1/06 ~ 5/2/06	5/1/06 12:20 PM	1	Deposition study
2334	Asphalt collection	5/1/06 ~ 5/2/06	5/1/06 12:20 PM	1	Deposition study
2335	Asphalt collection	5/1/06 ~ 5/2/06	5/1/06 12:20 PM	1	Deposition study
2336	Asphalt collection	5/1/06 ~ 5/2/06	5/1/06 12:20 PM	1	Deposition study
2341	Asphalt collection	5/17/06 ~ 5/18/06	5/17/06 12:10 PM	1	Deposition study
2342	Asphalt collection	5/17/06 ~ 5/18/06	5/17/06 12:10 PM	1	Deposition study
2343	Asphalt collection	5/17/06 ~ 5/18/06	5/17/06 12:10 PM	1	Deposition study
2344	Asphalt collection	5/17/06 ~ 5/18/06	5/17/06 12:10 PM	1	Deposition study
2345	Asphalt collection	5/17/06 ~ 5/18/06	5/17/06 12:10 PM	1	Deposition study
2346	Asphalt collection	5/17/06 ~ 5/18/06	5/17/06 12:10 PM	1	Deposition study
2311	Asphalt collection	4/6/06 ~ 4/7/06			Background blank
2331	Asphalt collection	5/1/06 ~ 5/2/06			Background blank
2341	Asphalt collection	5/17/06 ~ 5/18/06			Background blank
2411	Labeling	3/30/06 ~ 4/1/06			Labeled silica used for 4/6/06 field test
2412	Labeling	4/19/06 ~ 4/21/06			Labeled silica used for 5/1/06 & 5/17/06 field test

Table A-3 Dysprosium results for resusepnsion and deposition study

		Total Mass (g)		Deployed Mass	Irridated sample	Sample	Dy mass(µg)		Blank Corrected	Area normalized	Size of
Sample ID	Parameters	Deployed	Collected	Dy labeled silica	mass(g)	Concentration (µg g^{-1})	Irradiated	Total	Mass (µg)	Depositon (µg m^{-2})	Sample vial
1111031	Dy	0.248	0.094	0.086	0.0803	583	46.8	54.8	54.8		Large
1112031	Dy	0.250	0.064	0.083	0.0564	445	25.1	28.5	28.5		Large
1113031	Dy	0.257	0.048	0.083	0.0391	441	17.2	21.3	21.3		Large
1114031	Dy	0.243	0.052	0.082	0.0457	268	12.3	14.0	14.0		Large
1115031	Dy	0.255	0.071	0.082	0.0553	464	25.6	32.9	32.9		Large
1116031	Dy	0.250	0.040	0.088	0.0323	567	18.3	22.9	22.8		Large
1121031	Dy	0.247	0.074	0.085	0.0547	391	21.4	28.9	28.8		Large
1122031	Dy	0.253	0.063	0.085	0.0557	313	17.4	19.7	19.7		Large
1123031	Dy	0.243	0.049	0.084	0.0359	551	19.8	26.9	26.9		Large
1124031	Dy	0.246	0.062	0.087	0.0563	452	25.4	27.8	27.8		Large
1125031	Dy	0.250	0.040	0.085	0.0289	321	9.3	12.9	12.9		Large
1126031	Dy	0.248	0.076	0.086	0.0641	230	14.7	17.5	17.5		Large
1131031	Dy	NS	NS	NS	NS	NS	NS	NS	NS		Large
1132031	Dy	0.350	0.073	0.106	0.0456	335	15.3	24.4	24.4		Large
1133031	Dy	0.306	0.085	0.108	0.0598	342	20.4	28.9	28.9		Large
1134031	Dy	0.326	0.131	0.109	0.104	390	40.6	51.2	51.2		Large
1135031	Dy	0.301	0.074	0.102	0.0512	529	27.1	39.0	39.0		Large
1141031	Dy	0.271	0.172	0.090	0.141	387	54.4	66.6	66.6		Large
1142031	Dy	0.280	0.134	0.090	0.0902	476	42.9	63.6	63.6		Large
1143031	Dy	0.288	0.186	0.090	0.160	363	58.2	67.5	67.5		Large
1144031	Dy	0.271	0.152	0.090	0.122	346	42.2	52.7	52.6		Large
1145031	Dy	0.273	0.093	0.092	0.0768	435	33.4	40.5	40.5		Large
1151031	Dy	0.302	0.220	0.099	0.197	316	62.1	69.7	69.7		Large
1152031	Dy	0.287	0.136	0.087	0.101	316	31.9	42.8	42.8		Large
1153031	Dy	0.283	0.164	0.092	0.133	380	50.6	62.2	62.2		Large
1154031	Dy	0.300	0.116	0.099	0.0939	361	33.9	42.0	42.0		Large
1155031	Dy	0.299	0.111	0.099	0.100	244	24.4	27.0	27.0		Large
1156031	Dy	0.300	0.148	0.101	0.124	275	34.0	40.6	40.6		Large
1161031	Dy	0.290	0.219	0.095	0.183	335	61.3	73.4	73.4		Large
1162031	Dy	0.297	0.056	0.099	0.0411	182	7.5	10.2	10.2		Large
1163031	Dy	0.302	0.134	0.098	0.107	328	35.2	44.0	44.0		Large
1164031	Dy	0.295	0.139	0.099	0.119	316	37.4	43.7	43.7		Large
1165031	Dy	0.297	0.149	0.097	0.127	288	36.6	42.8	42.8		Large
1166031	Dy	0.310	0.161	0.100	0.142	264	37.4	42.4	42.4		Large
1411011	AD				0.0391	1.51	0.0590				Small
1412011	AD1				0.0388	1.58	0.0611				Small
1311021	BK *		0.607		ND	ND	ND	ND	ND		Small
1312021	BK1 *		1.19		ND	ND	ND	ND	ND		Small
1411041	DL				0.0210	1470	30.9				Small
1412041	DL1				0.0198	1360	26.9				Small
1411141	PB				0.0244	0.174	0.00424				Small
1412141	PB1				0.0251	0.191	0.00479				Small
1411151	P *				0.0190	0.0687	0.00130				Small
1111191	SC	0.249	0.150	0.0858	0.0340	95.7	3.25	14.4	14.4		Small
1112191	SC1				0.0336	104	3.50	15.6	15.6		Small
1411051	SD				0.0207	4.89	0.1011				Small
1411181	SO				0.0411	2.89	0.1186				Small
1412181	SO1				0.0445	2.84	0.1263				Small
1411061	STD				0.0577	5.46	0.3151				Large
1431011	AD				0.0407	1.22	0.0497				Small
1431171	B *				0.280	0.00327	0.000916				Small
1431161	BV				3.71	0.00408	0.0151				Large
1331021	BK		0.292		0.0463	2.22	0.103	0.649	0.648	20.0	Small
1332021	BK1		0.285		0.0562	1.59	0.0896	0.455	0.454	14.0	Small
1431041	DL				0.0218	2400	52.3				Small
1432041	DL1				0.0205	2280	46.7				Small
1431151	P *				0.0239	0.0546	0.00130				Small
1431141	PB				0.0211	0.423	0.00892				Small
1432141	PB1				0.0223	0.277	0.00617				Small
1131191	SC	0.301	0.219	0.100	0.0225	208	4.68	45.5	45.5		Small
1132191	SC1				0.0204	206	4.20	45.0	45.0		Small
1431051	SD				0.0216	4.67	0.101				Small
1431181	SO				0.0358	5.66	0.203				Small
1431061	STD				0.116	2.72	0.315				Large
1451011	AD *				0.0285	1.78	0.0506				Small
1451171	B *				0.278	0.00489	0.00136				Small
1351021	BK *		0.609		0.0478	1.41	0.0675	0.860	0.859	26.5	Small
1352021	BK1 *				0.0461	1.15	0.0531	0.701	0.700	21.6	Small
1451041	DL				0.0212	1620	34.3				Small
1452041	DL1				0.0234	1650	38.6				Small
1451151	P *				0.0236	0.110	0.00258				Small
1451141	PB *				0.0254	0.601	0.0153				Small
1452141	PB1 *				0.0217	0.602	0.0131				Small
1152191	SC	0.302	0.169	0.100	0.115	489	56.5	82.5	82.5		Large
1451051	SD				0.0223	5.44	0.121				Small
1451181	SO *				0.0265	3.54	0.0937				Small
1451061	STD				0.115	3.10	0.355				Large
2211031	Dy *						0.0275		0.012	1.23	Large
2212031	Dy *						0.00612		ND	ND	Large
2213031	Dy *						0.0125		ND	ND	Large
2214031	Dy *						0.00585		ND	ND	Large
2215031	Dy *						0.0121		ND	ND	Large
2216031	Dy *						0.00794		ND	ND	Large
2221031	Dy						0.0149		ND	ND	Large
2222031	Dy *						0.0129		ND	ND	Large
2223031	Dy *						0.0323		0.0171	1.71	Large
2224031	Dy *						0.0259		0.0107	1.07	Large
2225031	Dy *						0.00641		ND	ND	Large
2226031	Dy *						0.00883		ND	ND	Large
2231031	Dy						0.0102		ND	ND	Large
2232031	Dy *						0.0137		ND	ND	Large
2233031	Dy *						0.00897		ND	ND	Large
2234031	Dy *						0.0130		ND	ND	Large
2235031	Dy *						0.0113		ND	ND	Large

Table A-3 Dysprosium results for resusepnsion and deposition study -continued

Sample ID	Parameters	Total Mass (g) Deployed	Collected	Deployed Mass Dy labeled silica	Irridated sample mass(g)	Sample Concentration (μg g^{-1})	Dy mass(μg) Irradiated	Total	Blank Corrected Mass (μg)	Area normalized Depositon (μg m^{-2})	Size of Sample vial
2236031	Dy *						0.0120		ND	ND	Large
2241031	Dy *						0.0185		0.00338	0.338	Large
2242031	Dy *						0.0200		0.00482	0.482	Large
2243031	Dy *						0.0227		0.00753	0.753	Large
2244031	Dy *						0.0163		0.00117	0.117	Large
2245031	Dy *						0.0126		ND	ND	Large
2246031	Dy *						0.0262		0.0111	1.11	Large
2311031	Dy *						0.00523		ND	ND	Large
2312031	Dy *						0.0952		0.0801	2.47	Large
2313031	Dy *						0.0499		0.0348	1.07	Large
2314031	Dy *						0.0989		0.0838	2.58	Large
2315031	Dy *						0.0517		0.0365	1.13	Large
2316031	Dy *						0.0568		0.0416	1.28	Large
2321031	Dy *						0.0024		ND	ND	Large
2322031	Dy *						0.0334		0.0183	0.563	Large
2323031	Dy *						0.0164		0.00129	0.0396	Large
2324031	Dy *						0.0256		0.0105	0.323	Large
2325031	Dy *						0.0416		0.0265	0.816	Large
2326031	Dy *						0.0526		0.0375	1.16	Large
2331031	Dy *						0.0413		ND	ND	Large
2332031	Dy *						0.212		0.147	4.55	Large
2333031	Dy *						0.158		0.094	2.89	Large
2334031	Dy *						0.235		0.171	5.26	Large
2335031	Dy *						0.142		0.077	2.39	Large
2336031	Dy *						0.374		0.310	9.56	Large
2341031	Dy *						0.0333		ND	ND	Large
2342031	Dy *						0.0664		0.00205	0.063	Large
2343031	Dy *						0.0765		0.0121	0.373	Large
2344031	Dy *						0.0696		0.00521	0.161	Large
2345031	Dy *						0.0541		ND	ND	Large
2346031	Dy *						0.0427		ND	ND	Large
2311021	BK *		0.227		0.0257	0.937	0.0241	0.213	0.198	6.09	Small
2312021	BK1 *		0.0992		0.0211	3.17	0.0669	0.315	0.299	9.24	Small
2211131	BLK *						0.00360				Large
2411041	DL				0.0202	2410	48.8				Small
2412041	DL1				0.0196	2380	46.7				Small
2111121	M	1.75	1.43	0.580	0.176	397	70.0	567	567		Large
2112121	M1	1.80	1.49	0.605	0.199	386	77.0	577	577		Large
2411141	PB *				0.0198	0.335	0.00663				Small
2412141	PB1 *				0.0221	0.543	0.0120				Small
2411051	SD				0.0230	6.14	0.141				Small
2411061	STD *				0.1160	3.41	0.396				Large
2411071	TF *				0.0148	0.285	0.00420				Large
2331021	BK *		0.278		0.0638	2.63	0.168	0.731	0.678	20.9	Small
2341021	BK *		0.328		0.0493	3.41	0.168	1.118	1.06	32.8	Small
2231131	BLK						0.00712				Large
2241131	BLK *						0.0103				Large
2431041	DL				0.0222	1920	42.5				Small
2432041	DL1				0.0205	1990	40.9				Small
2131121	M	0.507	0.292	0.169	0.0282	456	12.9	133	133		Small
2132121	M1	1.70	0.800	0.568	0.0297	725	21.5	580	580		Small
2431141	PB *				0.0213	0.586	0.0125				Small
2432141	PB1 *				0.0226	0.942	0.0213				Small
2431051	SD				0.0233	4.94	0.115				Small
2431061	STD *						0.315				Large
2431071	TF *						0.0644				Large

Table A-4 Iridium results for resusepnsion and deposition study

Sample ID	Parameters	Total Mass (g) Deployed	Collected	Deployed Mass Ir labeled silica	Irridated sample mass(g)	Sample Concentration (µg g^{-1})	Ir mass(µg) Irradiated	Total	Blank Corrected Mass (µg)	Area normalized Depositon (µg m^{-2})	Size of Sample vial
1111082	Ir	0.248	0.0939	0.0764	0.0803	13.3	1.07	1.25	1.25		Large
1112082	Ir	0.250	0.0641	0.0817	0.0564	8.99	0.507	0.576	0.570		Large
1113082	Ir	0.257	0.0484	0.0794	0.0391	10.7	0.417	0.516	0.510		Large
1114082	Ir	0.243	0.0521	0.0833	0.0457	15.2	0.694	0.791	0.786		Large
1115082	Ir	0.255	0.0710	0.0860	0.0553	11.4	0.629	0.808	0.802		Large
1116082	Ir	0.250	0.0403	0.0755	0.0323	11.1	0.358	0.447	0.441		Large
1121082	Ir	0.247	0.0738	0.0815	0.0547	13.5	0.741	0.999	0.993		Large
1122082	Ir	0.253	0.0629	0.0893	0.0557	8.72	0.486	0.548	0.542		Large
1123082	Ir	0.243	0.0488	0.0787	0.0359	11.3	0.407	0.554	0.548		Large
1124082	Ir	0.246	0.0615	0.0747	0.0563	10.0	0.560	0.612	0.606		Large
1125082	Ir	0.250	0.0403	0.0828	0.0289	9.72	0.281	0.392	0.386		Large
1126082	Ir	0.248	0.0763	0.0766	0.0641	10.1	0.650	0.774	0.768		Large
1131082	Ir	NS	NS	NS	NS	NS	NS	NS	NS		Large
1132082	Ir	0.350	0.0729	0.0965	0.0456	13.5	0.617	0.988	0.982		Large
1133082	Ir	0.306	0.0846	0.0983	0.0598	23.4	1.40	1.98	1.97		Large
1134082	Ir	0.326	0.131	0.112	0.104	30.3	3.16	3.98	3.97		Large
1135082	Ir	0.301	0.0736	0.103	0.0512	26.0	1.33	1.91	1.91		Large
1141082	Ir	0.271	0.172	0.0947	0.141	49.4	6.94	8.50	8.50		Large
1142082	Ir	0.280	0.134	0.0903	0.0902	30.7	2.76	4.09	4.09		Large
1143082	Ir	0.288	0.186	0.104	0.160	45.9	7.36	8.54	8.53		Large
1144082	Ir	0.271	0.152	0.0918	0.122	43.1	5.25	6.56	6.55		Large
1145082	Ir	0.273	0.0932	0.0886	0.0768	32.7	2.51	3.04	3.04		Large
1151082	Ir	0.302	0.220	0.0946	0.197	4.18	0.821	0.920	0.914		Large
1152082	Ir	0.287	0.136	0.0968	0.101	4.50	0.454	0.609	0.603		Large
1153082	Ir	0.283	0.164	0.0935	0.133	3.34	0.445	0.548	0.542		Large
1154082	Ir	0.300	0.116	0.102	0.0939	4.03	0.379	0.469	0.463		Large
1155082	Ir	0.299	0.111	0.101	0.100	3.11	0.311	0.345	0.339		Large
1156082	Ir	0.300	0.148	0.100	0.124	3.72	0.460	0.548	0.542		Large
1161082	Ir	0.290	0.219	0.0961	0.183	4.01	0.734	0.880	0.874		Large
1162082	Ir	0.297	0.0561	0.0973	0.0411	4.70	0.193	0.264	0.258		Large
1163082	Ir	0.302	0.134	0.101	0.107	3.33	0.358	0.448	0.442		Large
1164082	Ir	0.295	0.139	0.0994	0.119	3.86	0.458	0.535	0.529		Large
1165082	Ir	0.297	0.149	0.102	0.127	2.93	0.372	0.436	0.430		Large
1166082	Ir	0.310	0.161	0.101	0.142	3.50	0.496	0.562	0.556		Large
1411012	AD				0.0391	0.00215	0.0000842				Small
1412012	AD1				0.0388	0.0678	0.00263				Small
1311022	BK		0.607		0.0790	0.00474	0.000374	0.00288	0.00243		Small
1312022	BK1		1.19		0.0789	0.0196	0.00154	0.0234	0.0229		Small
1411092	IL				0.0287	34.2	0.983				Small
1412092	IL1				0.0283	31.1	0.879				Small
1411142	PB				0.0244	0.0508	0.00124				Small
1412142	PB1				0.0251	0.0213	0.000534				Small
1411152	P				0.0260	0.219	0.00569				Small
1111192	SC	0.249	0.150	0.0782	0.0336	11.3	0.378	1.69	1.69		Small
1112192	SC1				0.034	10.2	0.345	1.52	1.52		Small
1411102	SI				0.0283	3.55	0.100				Small
1411182	SO				0.0411	0.0219	0.000902				Small
1412182	SO1				0.0445	0.00807	0.000359				Small
1411112	STI				0.0765	4.00	0.306				Large
1431012	AD				0.0407	0.00638	0.000260				Small
1431172	B				0.280	0.00262	0.000732				Small
1431162	BV				3.71	0.00159	0.00589				Large
1331022	BK		0.292		0.0463	0.00555	0.000257	0.00162	0.00118	0.0362	Small
1332022	BK1		0.285		0.0562	0.00452	0.000254	0.00129	0.000844	0.0260	Small
1431092	IL				0.0231	115	2.67				Small
1432092	IL1				0.0221	118	2.60				Small
1431152	P				0.0230	0.0169	0.000389				Small
1431142	PB				0.0211	0.0148	0.000313				Small
1432142	PB1				0.0223	0.00982	0.000219				Small
1131192	SC	0.301	0.219	0.0996	0.0225	44.0	0.989	9.61	9.61		Small
1132192	SC1				0.0204	51.9	1.06	11.3	11.3		Small
1431102	SI				0.0226	4.43	0.100				Small
1431182	SO *				0.0358	0.0397	0.00142				Small
1431112	STI				0.113	2.64	0.299				Large
1451012	AD *				0.0285	0.0243	0.000694				Small
1451172	B *				0.278	0.000562	0.000156				Small
1351022	BK *		0.609		0.0478	0.000631	0.0000301	0.000384	ND	ND	Small
1352022	BK1 *				0.0461	0.00405	0.000187	0.002	0.002	0.0623	Small
1451092	IL				0.0267	12.0	0.319				Small
1452092	IL1				0.0272	12.1	0.328				Small
1451152	P *				0.0243	0.00372	0.000090				Small
1451142	PB *				0.0254	0.0109	0.000276				Small
1452142	PB1 *				0.0217	0.0337	0.000732				Small
1152192	SC	0.302	0.169	0.102	0.115	3.53	0.407	0.595	0.589		Large
1451102	SI				0.0217	4.64	0.101				Small
1451182	SO *				0.0265	0.00872	0.000231				Small
1451112	STI				0.113	2.96	0.336				Large
2211082	Ir						0.0230		0.0171	1.71	Large
2212082	Ir *						0.00208		ND	ND	Large
2213082	Ir						0.00534		ND	ND	Large
2214082	Ir						0.00364		ND	ND	Large
2215082	Ir						0.00324		ND	ND	Large
2216082	Ir						0.00246		ND	ND	Large
2221082	Ir						0.0356		0.0297	2.97	Large
2222082	Ir *						0.00317		ND	ND	Large
2223082	Ir						0.00401		ND	ND	Large
2224082	Ir						0.00465		ND	ND	Large
2225082	Ir						0.00770		0.00180	0.180	Large
2226082	Ir						0.00312		ND	ND	Large
2231082	Ir						0.00240		ND	ND	Large
2232082	Ir						0.00328		ND	ND	Large
2233082	Ir						0.00245		ND	ND	Large
2234082	Ir						0.00249		ND	ND	Large
2235082	Ir						0.00213		ND	ND	Large

Table A-4 Iridium results for resusepnsion and deposition study-continued

Sample ID	Parameters	Total Mass (g) Deployed	Collected	Deployed Mass Ir labeled silica	Irridated sample mass(g)	Sample Content (µg/g)	Ir mass(µg) Irradiated	Total	Blank(filter+vial) Corrected Mass (ug)	Area normalized Depositon (µg/m^2)	Size of Sample vial
2236082	Ir						0.00221		ND	ND	Large
2241082	Ir						0.00467		ND	ND	Large
2242082	Ir						0.00303		ND	ND	Large
2243082	Ir						0.00251		ND	ND	Large
2244082	Ir						0.00233		ND	ND	Large
2245082	Ir						0.00226		ND	ND	Large
2246082	Ir						0.00290		ND	ND	Large
2311082	Ir						0.00138		ND	ND	Large
2312082	Ir						0.00264		ND	ND	Large
2313082	Ir						0.00192		ND	ND	Large
2314082	Ir						0.00103		ND	ND	Large
2315082	Ir						0.00218		ND	ND	Large
2316082	Ir						0.00114		ND	ND	Large
2321082	Ir						0.00132		ND	ND	Large
2322082	Ir						0.00102		ND	ND	Large
2323082	Ir						0.00134		ND	ND	Large
2324082	Ir						0.00456		ND	ND	Large
2325082	Ir						0.00147		ND	ND	Large
2326082	Ir						0.00126		ND	ND	Large
2331082	Ir						0.00293		ND	ND	Large
2332082	Ir						0.00354		ND	ND	Large
2333082	Ir						0.00158		ND	ND	Large
2334082	Ir						0.0300		0.0241	0.743	Large
2335082	Ir						0.0216		0.0157	0.485	Large
2336082	Ir						0.0465		0.0406	1.25	Large
2341082	Ir						0.00120		ND	ND	Large
2342082	Ir						0.00226		ND	ND	Large
2343082	Ir						0.00156		ND	ND	Large
2344082	Ir						0.00098		ND	ND	Large
2345082	Ir						0.00156		ND	ND	Large
2346082	Ir						0.000827		ND	ND	Large
2311022	BK *		0.227		0.0257	0.000216	0.00000556	0.0000491	ND	ND	Small
2312022	BK1 *		0.0992		0.0211	0.00256	0.0000541	0.000254	ND	ND	Small
2211132	BLK						0.00312		ND		Large
2411092	IL				0.0216	18.7	0.404				Small
2412092	IL1				0.0160	26.4	0.422				Small
2111122	M	1.75	1.43	0.586	0.176	9.69	1.71	13.8	13.8		Large
2112122	M1	1.80	1.49	0.594	0.199	10.0	1.99	14.9	14.9		Large
2411142	PB				0.0221	0.0223	0.000493				Small
2412142	PB1				0.0198	0.00195	0.0000387				Small
2411102	SI				0.0231	4.35	0.100				Small
2411112	STI						0.336				Large
2411072	TF						0.000497				Large
2331022	BK *		0.278		0.0638	0.000649	0.0000414	0.000180	ND	ND	Small
2341022	BK		0.328		0.0492	0.00593	0.000292	0.00194	0.000356	0.0110	Small
2231132	BLK						0.00345				Large
2241132	BLK						0.00269				Large
2431092	IL				0.0222	33.4	0.741				Small
2432092	IL1				0.0227	32.2	0.732				Small
2131122	M	0.507	0.292	0.169	0.0282	9.92	0.280	2.90	2.90		Small
2132122	M1	1.70	0.800	0.567	0.0297	10.6	0.314	8.47	8.47		Small
2431142	PB				0.0213	0.00852	0.000181				Small
2432142	PB1				0.0226	0.0203	0.000459				Small
2431102	SI				0.0269	3.73	0.100				Small
2431112	STI						0.306				Large
2431072	TF						0.00504				Large

Table A-5 24 hour average meteorological data

Sample ID	Time period	Type	Temp (℃)	Humidity (%)	Pressure (pa)	Wind Dir. (degree)	Wind Speed (m/s)	Wind Speed max(m/s)	Rain (cm)	Note
151 ~ 152	1/9/06 ~ 1/10/06	Mean	13.6	37.8	29.2	253	1.2	2.7	0.0	
151 ~ 152	1/9/06 ~ 1/10/06	Max	23.9	64.0	29.3	360	5.8	9.8	0.0	
151 ~ 152	1/9/06 ~ 1/10/06	Min	5.0	18.0	29.1	10	0.0	0.0	0.0	
151 ~ 152	1/10/06 ~ 1/11/06	Mean	14.3	34.7	29.1	91	1.2	2.5	0.0	
151 ~ 152	1/10/06 ~ 1/11/06	Max	24.4	52.0	29.2	360	2.2	5.4	0.0	
151 ~ 152	1/10/06 ~ 1/11/06	Min	7.8	16.0	29.0	10	0.0	0.4	0.0	
151 ~ 152	1/11/06 ~ 1/12/06	Mean	13.5	52.8	29.1	120	1.2	2.4	0.0	
151 ~ 152	1/11/06 ~ 1/12/06	Max	22.2	79.0	29.2	360	2.2	4.0	0.0	
151 ~ 152	1/11/06 ~ 1/12/06	Min	7.2	20.0	29.0	10	0.0	0.0	0.0	
151 ~ 152	1/12/06 ~1/13/06	Mean	15.3	44.6	29.1	94	1.1	2.4	0.0	25.17 hrs of time period
151 ~ 152	1/12/06 ~1/13/06	Max	24.4	62.0	29.2	320	2.2	6.3	0.0	25.17 hrs of time period
151 ~ 152	1/12/06 ~1/13/06	Min	9.4	19.0	28.9	20	0.0	0.0	0.0	25.17 hrs of time period
153 ~ 154	2/8/2006	Mean	27.8	8.8	28.9	100	2.0	4.8	0.0	9.17 hrs of time period
153 ~ 154	2/8/2006	Max	30.6	10.0	29.0	280	3.6	7.6	0.0	9.17 hrs of time period
153 ~ 154	2/8/2006	Min	24.4	8.0	28.8	10	0.4	1.8	0.0	9.17 hrs of time period
155 ~ 156	3/14/06 ~ 3/15/06	Mean	11.5	64.9	29.1	179	1.3	3.0	0.0	
155 ~ 156	3/14/06 ~ 3/15/06	Max	19.4	97.0	29.3	360	4.5	6.7	0.0	
155 ~ 156	3/14/06 ~ 3/15/06	Min	3.9	27.0	29.0	10	0.0	0.0	0.0	
155 ~ 156	3/15/06 ~ 3/16/06	Mean	11.1	63.0	29.2	125	0.9	2.3	0.0	25.15 hrs of time period
155 ~ 156	3/15/06 ~ 3/16/06	Max	18.3	91.0	29.3	360	2.7	7.2	0.0	25.15 hrs of time period
155 ~ 156	3/15/06 ~ 3/16/06	Min	5.0	36.0	29.1	10	0.0	0.0	0.0	25.15 hrs of time period
251~252	4/6/06 ~4/7/06	Mean	12.7	71.8	29.1	164	1.0	2.5	0.0	24.67 hrs of time period
251~252	4/6/06 ~4/7/06	Max	19.4	99.0	29.2	360	2.7	5.8	0.0	24.67 hrs of time period
251~252	4/6/06 ~4/7/06	Min	6.1	41.0	29.0	10	0.0	0.0	0.0	24.67 hrs of time period
253	5/1/06 ~ 5/2/06	Mean	18.6	76.4	28.9	238	1.2	2.7	0.0	
253	5/1/06 ~ 5/2/06	Max	28.3	98.0	29.0	360	2.2	4.5	0.0	
253	5/1/06 ~ 5/2/06	Min	12.8	44.0	28.8	10	0.0	0.0	0.0	
254	5/17/2006	Mean	21.9	70.0	28.9	272	1.3	2.8	0.0	
254	5/17/2006	Max	31.7	95.0	29.0	360	3.1	5.8	0.0	
254	5/17/2006	Min	15.6	42.0	28.7	50	0.0	0.0	0.0	

Table A-6 An example of meteorological data in the original format

Date	Time	Temp(F)	Hum(%)	DewT	Baro	WDir	WSpd(mph)	Wsmax(mph)	Solar	Rain
1/9/06	11:40	74	22	33	29.14	320	8	18	400	0
1/9/06	11:50	73	23	33	29.14	310	8	16	400	0
1/9/06	12:00	72	24	33	29.14	310	11	17	400	0
1/9/06	12:10	72	23	32	29.13	310	10	17	400	0
1/9/06	12:20	72	22	31	29.13	320	11	17	400	0
1/9/06	12:30	71	21	29	29.13	330	13	21	400	0
1/9/06	12:40	71	20	28	29.13	320	12	22	390	0
1/9/06	12:50	71	20	28	29.13	320	12	20	390	0
1/9/06	13:00	72	20	29	29.12	320	11	19	380	0
1/9/06	13:10	72	20	29	29.11	320	11	18	370	0
1/9/06	13:20	72	20	29	29.11	320	11	20	360	0
1/9/06	13:30	72	20	29	29.11	320	11	18	350	0
1/9/06	13:40	72	20	29	29.11	320	10	16	350	0
1/9/06	13:50	73	20	29	29.11	320	9	16	330	0
1/9/06	14:00	73	20	29	29.11	310	10	17	320	0
1/9/06	14:10	72	20	29	29.11	320	10	16	310	0
1/9/06	14:20	72	21	31	29.11	320	11	18	300	0
1/9/06	14:30	71	20	28	29.1	320	10	18	280	0
1/9/06	14:40	71	21	29	29.1	320	10	17	270	0
1/9/06	14:50	72	20	29	29.11	320	10	16	250	0
1/9/06	15:00	72	21	31	29.1	320	8	14	240	0
1/9/06	15:10	72	21	31	29.1	310	9	13	220	0
1/9/06	15:20	71	21	29	29.11	310	10	16	200	0
1/9/06	15:30	71	21	29	29.11	310	9	13	180	0
1/9/06	15:40	71	22	31	29.11	310	7	11	170	0
1/9/06	15:50	70	22	29	29.11	310	7	10	150	0
1/9/06	16:00	70	22	29	29.11	310	6	10	130	0
1/9/06	16:10	70	22	29	29.11	300	6	10	110	0
1/9/06	16:20	69	23	29	29.12	300	5	9	90	0
1/9/06	16:30	68	24	29	29.12	310	6	9	60	0
1/9/06	16:40	68	25	31	29.13	320	6	10	30	0
1/9/06	16:50	67	25	31	29.14	320	5	9	10	0
1/9/06	17:00	66	26	31	29.15	310	5	9	0	0
1/9/06	17:10	65	30	33	29.16	290	0	4	0	0
1/9/06	17:20	64	32	33	29.18	310	1	4	0	0
1/9/06	17:30	63	33	33	29.19	290	1	3	0	0
1/9/06	17:40	62	28	29	29.19	310	3	5	0	0
1/9/06	17:50	62	27	28	29.19	300	4	9	0	0
1/9/06	18:00	62	28	29	29.2	320	4	8	0	0
1/9/06	18:10	62	27	28	29.2	320	5	9	0	0
1/9/06	18:20	61	26	26	29.2	330	5	10	0	0
1/9/06	18:30	61	27	28	29.21	340	4	10	0	0
1/9/06	18:40	61	28	28	29.21	340	3	8	0	0
1/9/06	18:50	61	29	29	29.21	340	3	8	0	0
1/9/06	19:00	60	33	31	29.22	40	2	4	0	0
1/9/06	19:10	59	32	29	29.23	40	1	5	0	0
1/9/06	19:20	58	35	31	29.23	340	0	3	0	0
1/9/06	19:30	57	36	31	29.24	340	1	3	0	0
1/9/06	19:40	57	38	32	29.25	340	0	3	0	0
1/9/06	19:50	56	36	29	29.26	340	0	3	0	0
1/9/06	20:00	55	36	29	29.26	340	0	3	0	0
1/9/06	20:10	55	39	31	29.26	340	0	3	0	0
1/9/06	20:20	54	37	29	29.26	340	1	3	0	0
1/9/06	20:30	54	42	32	29.27	20	1	4	0	0
1/9/06	20:40	54	39	29	29.27	20	1	3	0	0
1/9/06	20:50	53	44	32	29.27	20	1	3	0	0
1/9/06	21:00	53	43	31	29.27	20	0	3	0	0
1/9/06	21:10	53	40	29	29.27	20	2	3	0	0
1/9/06	21:20	52	41	29	29.28	10	1	4	0	0
1/9/06	21:30	52	45	32	29.28	340	0	3	0	0
1/9/06	21:40	51	48	32	29.29	340	0	2	0	0
1/9/06	21:50	51	42	29	29.29	340	0	3	0	0
1/9/06	22:00	51	40	28	29.29	340	0	3	0	0
1/9/06	22:10	51	44	31	29.29	20	1	3	0	0
1/9/06	22:20	50	46	31	29.3	20	0	3	0	0
1/9/06	22:30	50	46	31	29.3	20	0	2	0	0
1/9/06	22:40	49	46	29	29.3	360	1	5	0	0
1/9/06	22:50	49	46	29	29.3	340	1	3	0	0
1/9/06	23:00	49	47	29	29.3	340	0	3	0	0
1/9/06	23:10	49	49	31	29.3	340	0	0	0	0
1/9/06	23:20	48	50	31	29.31	340	0	3	0	0
1/9/06	23:30	47	51	29	29.31	340	0	2	0	0
1/9/06	23:40	47	51	29	29.31	340	0	2	0	0
1/9/06	23:50	47	50	29	29.31	70	1	5	0	0